Developmental Biology 445 (2019) 189–210

Contents lists available at ScienceDirect

Developmental Biology

journal homepage: www.elsevier.com/locate/developmentalbiology

Original research article

Morphological, cellular and molecular characterization of posterior regeneration in the marine annelid *Platynereis dumerilii*

Anabelle Planques[a], Julien Malem[a], Julio Parapar[b], Michel Vervoort[a,*], Eve Gazave[a,*]

[a] Institut Jacques Monod, CNRS, UMR 7592, Université Paris Diderot, Sorbonne Paris Cité, F-75205 Paris, France
[b] Departamento de Bioloxía, Universidade da Coruña, Rúa da Fraga 10, 15008 A Coruña, Spain

ARTICLE INFO

Keywords:
Regeneration
Annelida
Stem cells
Platynereis dumerilii
Blastema
Cell proliferation
Dedifferentiation

ABSTRACT

Regeneration, the ability to restore body parts after an injury or an amputation, is a widespread but highly variable and complex phenomenon in animals. While having fascinated scientists for centuries, fundamental questions about the cellular basis of animal regeneration as well as its evolutionary history remain largely unanswered. Here, we present a study of regeneration of the marine annelid *Platynereis dumerilii*, an emerging comparative developmental biology model, which, like many other annelids, displays important regenerative abilities. When *P. dumerilii* worms are amputated, they are able to regenerate the posteriormost differentiated part of their body and a stem cell-rich growth zone that allows the production of new segments replacing the amputated ones. We show that posterior regeneration is a rapid process that follows a well reproducible path and timeline, going through specific stages that we thoroughly defined. Wound healing is achieved one day after amputation and a regeneration blastema forms one day later. At this time point, some tissue specification already occurs, and a functional posterior growth zone is re-established as early as three days after amputation. Regeneration timing is only influenced, in a minor manner, by worm size. Comparable regenerative abilities are found for amputations performed at different positions along the antero-posterior axis of the worm, except when amputation planes are very close to the pharynx. Regenerative abilities persist upon repeated amputations without important alterations of the process. We also show that intense cell proliferation occurs during regeneration and that cell divisions are required for regeneration to proceed normally. Finally, 5-ethynyl-2'-deoxyuridine (EdU) pulse and chase experiments suggest that blastemal cells mostly derive from the segment immediately abutting the amputation plane. The detailed characterization of *P. dumerilii* posterior body regeneration presented in this article provides the foundation for future mechanistic and comparative studies of regeneration in this species.

1. Introduction

Regeneration, the replacement of lost body parts, restoring mass and function (Poss, 2010), is a widespread phenomenon in metazoans (Bely and Nyberg, 2009). Regeneration occurs during the life of most if not all animals to replace cells that have been lost in minor day-to-day damages, in particular in tissues such as the epidermis and the epithelial lining of the gut ('homeostatic regeneration'; Poss, 2010). Regeneration can also occur after trauma, such as amputations or ablations ('injury-induced regeneration'; Poss, 2010). The extant of what can be regenerated after an injury varies a lot among animals: it can be only some cells (or even cell parts such as neuron axons), some tissues (such as the epidermis), some organs (such as the liver), some complex body structures (such as appendages) or even most or all of the body from a piece of tissue (Bely and Nyberg, 2009; Grillo et al., 2016). The ability to regenerate complex body structures, while not found in the most commonly studied animal model such as mammals, *Drosophila melanogaster* and *Caenorhabditis elegans*, is nevertheless found in species that belong to all the main branches of the metazoan tree, raising the possibility that this ability is an ancestral feature of animals and might therefore rely on homologous mechanisms and genetic networks (Bely and Nyberg, 2009).

Two main modes of regeneration have been generally described: epimorphic regeneration that requires active cell proliferation and morphallactic regeneration during which the restoration of the missing body part is solely due to the remodeling of pre-existing cell tissues (Morgan, 1901). In many cases, for example whole-body regeneration in planarians or limb regeneration in arthropods and vertebrates, epimorphic regeneration involves the formation of a regeneration-specific structure, the blastema (Sanchez Alvarado and Tsonis, 2006;

* Corresponding authors.
E-mail addresses: michel.vervoort@ijm.fr (M. Vervoort), eve.gazave@ijm.fr (E. Gazave).

https://doi.org/10.1016/j.ydbio.2018.11.004
Received 27 June 2018; Received in revised form 29 October 2018; Accepted 8 November 2018
Available online 13 November 2018

Poss, 2010; Tanaka, 2016). This structure is made of a superficial layer of epithelial cells that delineates an inner mass of mesenchyme-like cells, and gives rise to the regenerated structures. A key question in the regeneration field is to determine whether blastemal cells derive from pre-existing (resident) stem cells present in the body before amputation and subsequently 'activated' by injuries, or are produced by dedifferentiation of differentiated cells at or close to the amputation site, or even a combination of both possibilities (Tanaka and Reddien, 2011). Another crucial question is whether blastemal cells (or at least some of them) have self-renewal capabilities (and could therefore be considered as stem cells) and are pluripotent or multipotent (tissue-restricted) stem/progenitor cells. Planarian regeneration, for example, involves neoblasts (slowly-dividing resident stem cells) which are found throughout the body of uninjured animals (Sanchez et al., 2006). Upon injury, neoblasts migrate to the amputation site and produce the regeneration blastema through intense cell divisions. Among several distinct categories of neoblasts present in the body of these flatworms, only a specific type, clonogenic neoblasts, were shown to be pluripotent (*e.g.*, Fincher et al., 2018; Reddien, 2013; Wagner et al., 2011; Zeng et al., 2018). Dependence of regeneration on resident pluripotent stem cells has also been suggested in other animals with whole-body regeneration abilities, such as cnidarians, sponges and colonial ascidians (reviewed in Knapp and Tanaka, 2012; Tanaka and Reddien, 2011). During vertebrate limb regeneration, in contrast, the blastema seems to only contain tissue-restricted progenitor/stem cells, mainly produced by dedifferentiation processes at or near the amputation site, although resident tissue-restricted stem cells (for example satellite cells) may also be involved (Tanaka, 2016).

Annelids (segmented worms), which are composed of two main clades, the Sedentaria and the Errantia (Struck et al., 2011), are among the animals that show the most important regenerative abilities (Bely, 2014; Özpolat and Bely, 2016). Upon amputation, many annelids are able to regenerate the posterior part of their body, their anterior part (including the head), or both. There is a long history of experimental and descriptive studies of regeneration in many annelid species and more recently cellular and molecular aspects of this process have been studied in a few species, including the Errantia *Alitta virens* and the Sedentaria *Pristina leidyi*, *Capitella teleta*, *Eisenia fetida*, and *Enchytraeus japonensis* (for review; Özpolat and Bely, 2016). Most studies aiming at defining the cellular origin of the regenerated region in annelids have suggested that this region mostly or exclusively originated from cells located at or close to the amputation site, probably through dedifferentiation events (*e.g.*, Boilly, 1965a, 1965b; Boilly, 1968a, 1968b, 1968c; Boilly, 1969a, 1969b, 1969c; reviewed in Bely, 2014). In one particular group of Sedentaria annelids, clitellates (earthworms for example), it has been suggested that cells migrating over a long distance contribute to the formation of a part of the regenerated region (*e.g.*, de Jong and Seaver, 2017; Herlant-Meewis, 1964; Myohara, 2012). Long distance migration of cells towards the amputation site has also been described in *P. leidyi*, but the identity of the cells and their possible contribution to regeneration have not been assessed (Zattara et al., 2016).

In this study, we investigated regeneration of the marine annelid worm *Platynereis dumerilii* (Audouin and Milne Edwards, 1833), which belongs to the Errantia clade, and which has proven to be very useful for large-scale evolutionary developmental comparisons (Raible and Tessmar-Raible, 2014; Williams and Jékely, 2016). *P. dumerilii* displays a complex life cycle (Fischer et al., 2010): embryonic and larval development lead in three days to the formation of a three-segment worms that will subsequently grow during most of their life, by sequentially adding new segments at their body posterior end, just before the pygidium. This process, known as posterior growth, relies on the presence of a subterminal 'growth zone' that contains stem/progenitor cells expressing a complex molecular signature, the Germline Multipotency Program (GMP; Juliano et al., 2010), also displayed by pluripotent/multipotent somatic stem cells and primordial germ cells in other animals (Gazave et al., 2013). *P. dumerilii* worms also have important regeneration abilities. When the posterior part of their body is amputated, which leads to the removal of the pygidium (final non-metameric part of the body), the growth zone and several segments, the worms are able to heal and then to regenerate the pygidium and the growth zone (a process that we refer to as posterior regeneration). These wound healing and regeneration phases are followed by post-regenerative posterior growth during which the regenerated growth zone produces new segments replacing the amputated ones (Gazave et al., 2013). When and how these different phases take place after amputation is, however, not known. In this article, we performed a detailed characterization of this regeneration process at the morphological, cellular and molecular levels. We found that *P. dumerilii* posterior regeneration is a rapid process that passes through well-defined and reproducible stages, which are conserved after multiple repeated amputations. Posterior regeneration involves the formation of a blastema-like structure and requires intense cell proliferation. EdU pulse and chase experiments suggest that the *P. dumerilii* blastema is mostly produced by cells of the differentiated segment abutting the amputation plane.

2. Materials and methods

2.1. Breeding culture and worm collection

P. dumerilii worms were obtained from a breeding culture established in the Institut Jacques Monod, according to the protocol of Dorresteijn et al. (1993). In most experiments, 3–4 months' worms with 30–40 segments were used. After anesthesia (with a solution of MgCl2 7.5% and sea water, 1/1), sharp amputations of the posteriormost part of the worms were done using a microknife (Sharpoint™) between two segments (perpendicularly to the body axis), in order to remove the 5–6 posteriormost segments and the pygidium. After amputation, worms were let to recover in fresh sea water and fed normally three times per week. For serial amputations, worms were amputated the 1st time as explained above and, for the following amputations, we removed the regenerated region and the adjacent differentiated segment, which implies a reduction in the worm size by one segment at each amputation. At defined time points after amputation, worms were fixed in 4% paraformaldehyde (PFA) in 100 mM PBS tween 0.1% (PTW) for 2 h at RT, washed with PTW and stored at − 20 °C in 100% MeOH for subsequent experiments. For phalloidin staining (see below), worms were similarly fixed in PFA and rinsed in PTW but were then directly stored at 4 °C for up to 4 days before labeling, without MeOH dehydration.

2.2. Micro-computed X-ray tomography (microCT) and scanning electron microscopy (SEM)

For microCT imaging, specimens were gradually dehydrated in ascending ethanol series up to 96% ethanol and then dehydrated for two hours with hexamethyldisilazane (HMDS) and left to dry overnight before scanning, following Alba-Tercedor and Sánchez-Tocino (2011). Scanning was carried out with a microtomograph Skyscan 1172 (Bruker, Belgium) using the following parameters: voltage 55 kv, current 165 uA, and pixel size between 0.54 and 1.28 µm depending on the sample size. No filter was used, and samples were rotated 360° for obtaining as much detail as possible. The X-ray projection images obtained during scannings were reconstructed with the software NRecon (Bruker, Belgium). The sections obtained were processed with the programmes CTAn and DataViewer (Bruker, Belgium). 3D representations were obtained with the programme CTVox (Bruker, Belgium). For Scanning Electron Microscopy (SEM) experiments, specimens were dehydrated *via* a graded ethanol series, prepared by critical-point drying using CO_2, mounted on aluminium stubs, covered with gold in a BALTEC SCD 004 evaporator, and examined and photographed under a JEOL JSM-6400 SEM.

2.3. Cloning of Pdum-piwiB and phylogenetic analysis of piwi genes

A previously unidentified *P. dumerilii piwi* gene (subsequently named *Pdum-piwiB*) was found by sequence similarity searches against the *P. dumerilii* transcriptomic database PdumBase (pdumbase.gdcb.iastate.edu; Chou et al., 2018). The gene was cloned using standard protocols as described in Gazave et al. (2013). Phylogenetic tree reconstruction was performed using the dataset of *piwi/argonaute* genes used by Kerner et al. (2011) to study the evolution of this large gene family in metazoans, and methods described in Gazave et al. (2013). Accession number of the newly cloned gene: MK089779.

2.4. Whole-mount in situ hybridizations (WMISH), immunolabelings, EdU cell proliferation assay, and imaging

Nitro blue tetrazolium chloride/ 5-brom-4-chloro-3'-indolyphosphate p-toluidine salt (NBT/BCIP) WMISH and immunolabelings were performed as previously described (Tessmar-Raible et al., 2005; Demilly et al., 2013; Gazave et al., 2017). For all labelings, after rehydration, samples were treated with 40 µg/ml proteinase K PTW for 10 min, 2 mg/ml glycine PTW for 1 min, 4% PFA PTW for 20 min and washed in PTW prior to hybridization or labeling. Immunolabelings were done as previously described (Demilly et al., 2013) using mouse anti-acetylated tubulin (Sigma T7451, 1:500) and fluorescent secondary anti-mouse IgG Alexa Fluor 488 or 555 conjugate (Invitrogen, 1:500) antibodies. For phalloidin labeling, digestion and post-fixation steps were done similarly on non-rehydrated samples that were subsequently incubated in phalloidin-Alexa 555 (Molecular Probes, 1:100) overnight with shaking at 4 °C.

Proliferating cells were labeled by incubating worms with the thymidine analog 5-ethynyl-2′-deoxyuridine (EdU), which was subsequently fluorescently labeled with the Click-It EdU Imaging Kit (488 or 555, Molecular Probes) as described in Demilly et al. (2013). Worms were incubated for 1 h or 5 h in sea water with 5 µM EdU. Various pulse and chase experiments were performed as described in the result section.

Following fluorescent labeling procedures, samples were counterstained with Hoechst (or DAPI) at 1 µg per ml and stored and mounted in 87% glycerol containing 2.5 mg/ml of anti-photobleaching reagent DABCO (Sigma, St. Louis, MO, USA) before confocal imaging.

Bright field images were taken on a Leica microscope for visible NBT/BCIP WMISH. In all figures with WMISH images, we show for stage 1 the whole last segment abutting the amputation site, including the wound epithelium, whereas for later stages only the regenerated region and the posteriormost part of the last segment are shown. For stage 1 to 4, for the sake of clarity, we chose not to materialize the position of the amputation plane on the images, which can nevertheless be easily positioned in the uppermost part of the pictures in the transition region between the wide last segment (on which part of parapodia and associated secreting glands displaying non-specific staining, can often be seen) and the much narrower regenerated region devoid of differentiated parapodia. Confocal images were taken with a Zeiss LSM 710 confocal microscope. Adjustment of brightness and contrast, Z projections were performed using ImageJ and Adobe Photoshop. The figure panels were compiled using Adobe Illustrator.

2.5. Cell proliferation inhibitor treatments

Cell proliferation during regeneration was blocked using two well characterized inhibitors, hydroxyurea (HU, Sigma H8627) and nocodazole (Sigma M1404). Nocodazole treatments, while blocking regeneration, induced high worm autotomy (self-amputation) and lethality (not shown), even at low concentration (0.01 µM, 0.1 µM and 1 µM), and therefore further experiments were done only with HU. HU was dissolved in sea water (10, 20 mM or 50 mM) and the HU solution was changed every 24 h to maintain its activity for the duration of the experiment. Worms were incubated in 2 ml of HU solution in 12-wells plate for the desired time period (see Results for details). We tested possible toxicity of HU by treating non-amputated worms with 20 mM HU and performing a daily observation of the worms. After five days of treatment, we observed that the 12 treated worms were alive (eight were completely normal, three displayed shortened anal cirri and one had undergone autotomy). After ten days of treatment, two animals had died, three had undergone autotomy and six had shortened anal cirri. Together with those made on regenerating animals (see Results), these observations suggest that 20 mM HU only has low toxicity, at least for treatments that do not exceed five days.

2.6. Scoring and statistical analyses

For morphological and HU treatment experiments, worms were observed under the dissecting microscope at different time points after amputation and 'scored'. Scoring was done according to the regeneration stage that has been reached (stages 1–5; see Results and Fig. 1 for the definition of stages) or the number of morphologically distinguishable segments (*i.e.*, with parapodia and clear segmental boundaries) that have been produced (X s., X being the number of visible segments). Some worms showed a morphology that was intermediate between that of two successive stages of regeneration and were therefore scored as 1.5, 2.5, 3.5, and 4.5.

Graphic representations of morphological experiments and statistical analyses were performed using the Prism 7 software (GraphPad). For group multiple comparisons (worm sizes and position of amputation experiments; Fig. 2), 2-way ANOVA on repeated measures using Tukey correction were used. For the study of worms' regeneration with daily scoring after four serial amputations (Fig. 3), 2-way ANOVA on 2 factors repeated measures using Dunnett correction was performed. Two worms died during the experiment and were thus removed from analysis, as was one worm whose score was missing for one day. For HU treatments (Fig. 9), 2-way ANOVA on repeated measures using Dunnett correction was performed. Comparisons with similar p-values were grouped for graphic representation.

3. Results

3.1. Definition of P. dumerilii posterior regeneration stages

We tested the regeneration abilities of juvenile worms that are in the post-larval growth phase of their life cycle during which they grow by adding new segments one by one from the posterior part of their body (posterior growth). This phase starts at the end of embryonic and larval development. At this time, the worms display a head, three segments with a pair of lateral appendages (parapodia), and a terminal body non-segmental element called the pygidium (Fig. 1A,G). Posterior growth ends when the worms become sexually-mature. In our worm culture conditions, this growth phase spans over from four months to a maximum of one year and a half and, toward the end, the worms are made of around 80 segments. While the number of segments of the worms increases with age, there is no strict correlation between the number of segments, the overall size and the age of the worms.

In a first set of experiments, worms long of 30–40 segments (3–4 month-old) were amputated of their pygidium (which bears the anus and characteristic bilateral outgrowths named anal cirri) and last five to six posterior segments. We then characterized their regeneration using three complementary imaging approaches, (i) scanning electron microscopy (SEM; Fig. 1A-F), which allows the description of the external morphology, (ii) micro-computed X-ray tomography (microCT; Fig. 1G-J'), which provides information about differentiated internal structures present in the regenerated region, and (iii) bright field microscopy (Fig. 1K-O), which enables to establish a quick visual staging method at the dissecting scope. We found that regeneration proceeds through five reproducible stages with a similar timing in most

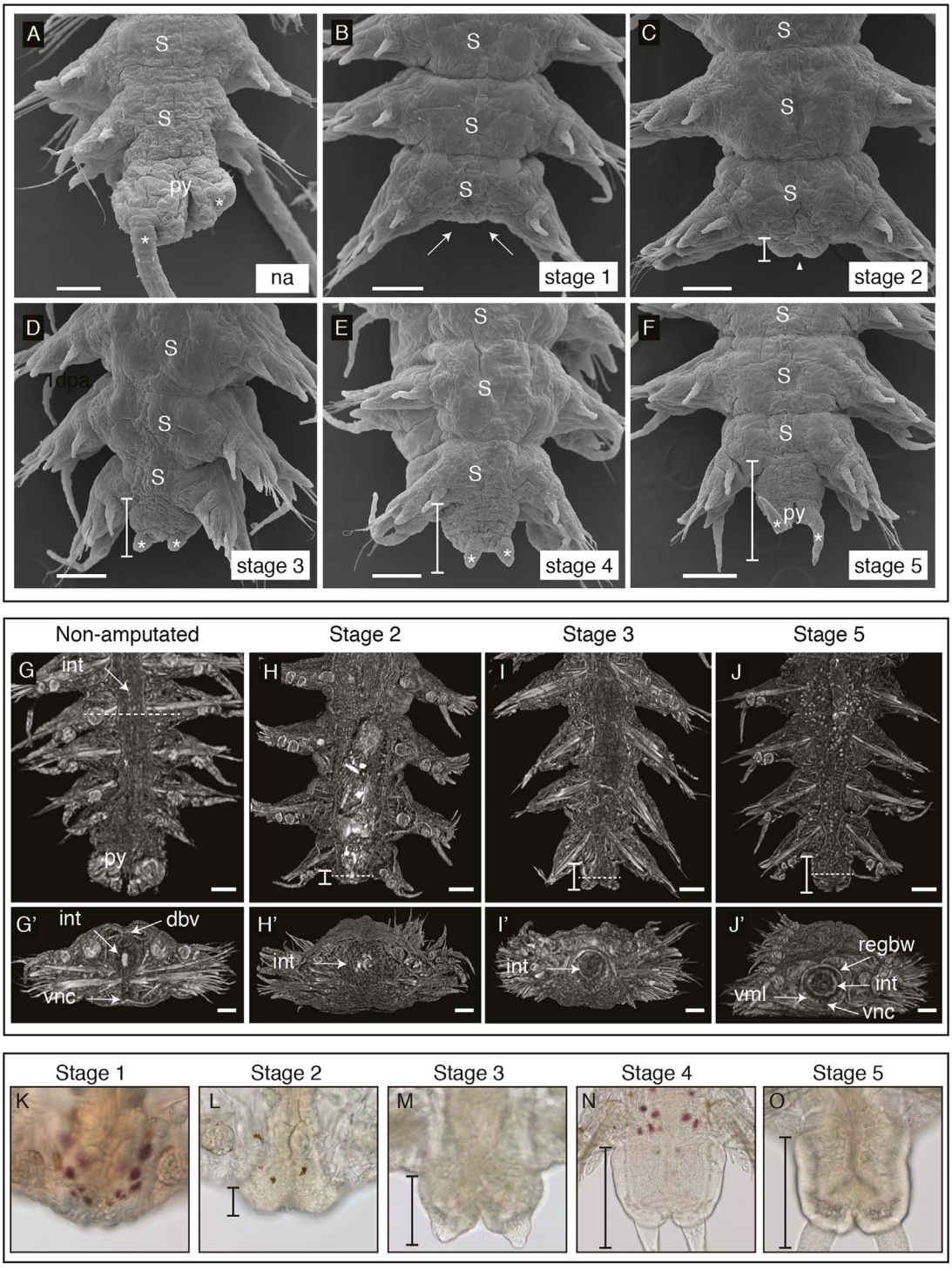

Fig. 1. Morphological characterization of posterior regeneration. (A-F) Scanning Electron Microscopy (SEM) micrographs of posterior regeneration stages. (A) Non-amputated (na) condition showing the posterior part of a worm including the last body segments (S) and the pygidium (py) bearing the anus and anal cirri (asterisks). Left anal cirrus is detached (right side, out of focus). (B) Stage 1 (1-day post amputation, 1 dpa): wound healing is achieved (white arrows) but no posterior outgrowth is present. (C) Stage 2 (2 dpa): a small regenerated region is visible (white bracket) with a notch in its central part (white arrowhead) that likely corresponds to the reformed anus. (D) Stage 3 (3 dpa): regenerated region has increased in size, and two small anal cirri are visible (asterisks). (E) Stage 4 (4 dpa): size of the regenerated region and anal cirri has increased as compared to the previous stage. (F) Stage 5 (5 dpa): an indentation separates the differentiating pygidium (bearing longer anal cirri) from the anterior part of the regenerated region. Right ventral cirrus is ventrally bent. All pictures are ventral views. Scale bars= 50 μm. White brackets delineate the regenerated region. S= segment; py= pygidium; asterisks= anal cirri; arrowhead = anus; arrows = wound epithelium. (G-J') Micro-computed X-ray tomography (microCT) images of posterior regeneration stages. G to I images correspond to mid-coronal sections of the posterior part of a non-amputated worm (G) and at different stages of regeneration (H-J). The dotted lines correspond to the virtual plan of the transversal sections shown in G' to J'. Brackets highlight the regenerated region in H to J. (G-G') In a non-amputated worm, several internal structures such as the intestine, dorsal and ventral blood vessels and ventral nerve cord can be seen. (H-I') At stage 2 and 3, only the intestine is distinguishable in the still very small regenerated region. (J-J') At stage 5, intestine, ventral nerve cord and ventral wall muscle layers can be distinguished in the regenerated region. int= intestine; py= pygidium; dbv= dorsal blood vessel; regbw= regenerated body wall; vml= ventral muscular layer; vnc= ventral nerve cord. Scale bars= 50 μm. (K-O) Bright-field microscopy images of the five stages of regeneration. Brackets highlight the regenerated region in L to O.

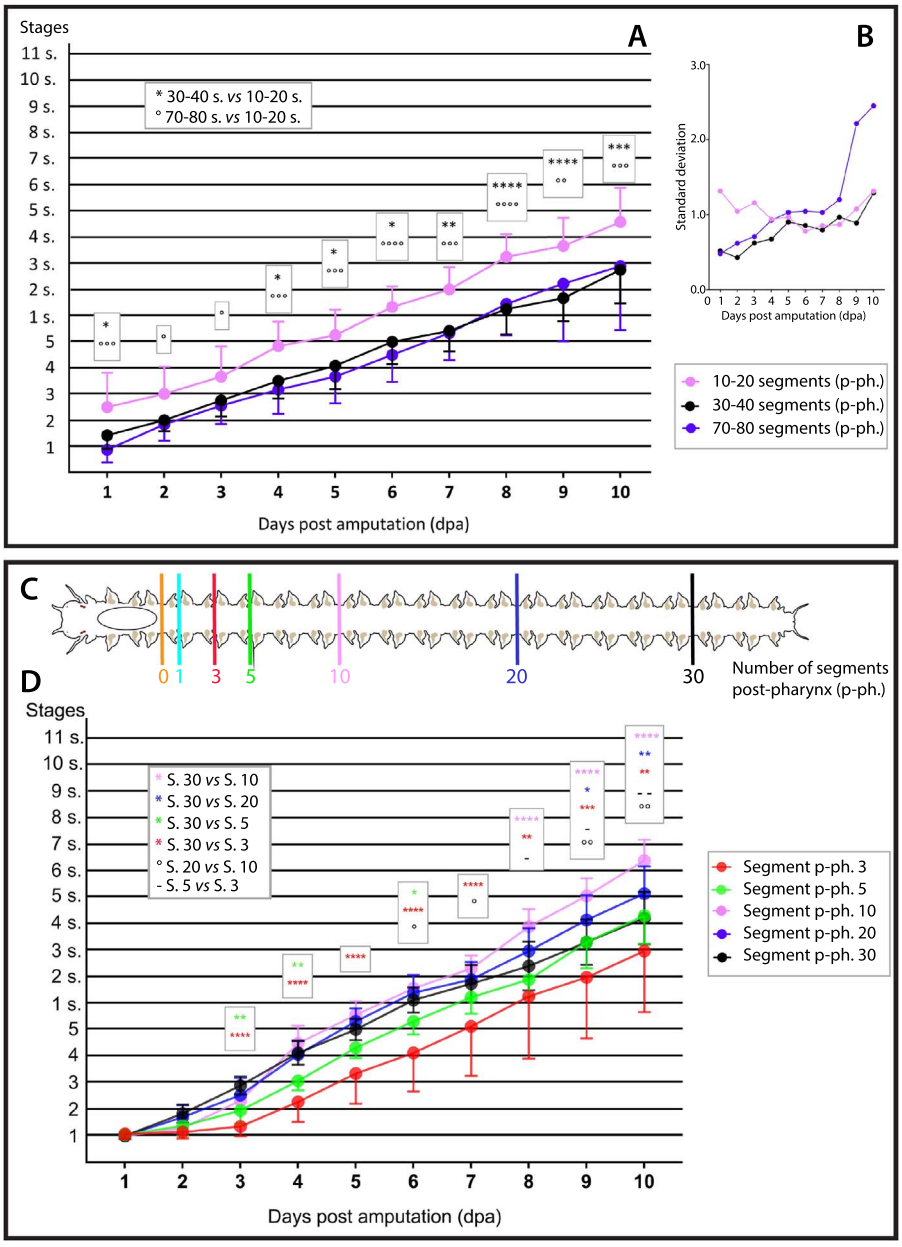

Fig. 2. Influence of worm size and position of the amputation plane on posterior regeneration. (A-B) Influence of worm size on posterior regeneration. Three categories of worms were used: worms with 10–20 post-pharynx segments (in pink, n = 12), worms with 30–40 post-pharynx segments (in black, n = 12) and worms with post-pharynx 70–80 segments (in blue, n = 18). (A) Graphic representation of the stages reached by the worms every day during ten days. Whereas complete regeneration and production of segments are observed in all three conditions, worms with 10–20 post-pharynx segments regenerate and thus produce segments significantly faster than the longer worms. 30–40 and 70–80 post-pharynx segments worms do not show significant difference in their timing of regeneration. (B) Graphic representation of the standard deviation (SD, used as a measure of inter-individual variability) of the stages reached by the worms during the ten days following amputation. The worms with 30–40 post-pharynx segments show the lowest variability during the whole process. (C and D) Influence of amputation plane position on posterior regeneration. Each amputation position is color-coded. (C) Schematic representation of the seven different positions of amputation along the worm body axis that have been tested. The position 0 corresponds to the location immediately posterior to the pharynx (schematized as an ellipse). Other positions correspond to the number of segments posteriorly to this position 0 (noted p-ph. for post-pharynx). (D) Graphic representation of the stages reached by the worms every day during ten days. At the exception of one worm amputated in position p-ph. 1 which has reached stage 4 after ten days, worms amputated at position 0 and p-ph. 1 died shortly after amputation without any sign of regeneration and are therefore not represented on the graph. Regeneration and segment addition occurred in the five other conditions. Worms amputated at position p-ph. 3 were significantly delayed as compared to worms amputated at position p-ph. 30 at day 3 and this delay was kept during all following days, while from stage 4 onwards these worms followed a normal regeneration timing of one stage or one segment per day. Four worms died during the experiment (one per day from day 2–4). Amputation at position p-ph. 5 led to a delayed regeneration at days 3, 4 and 6, as compared to worms amputated at position p-ph. 30, but there was no more significant difference during the four following days. Worms amputated at position p-ph. 3 and p-ph. 5 showed significant differences only during segment addition, from day 8 onwards. Positions p-ph. 10, p-ph. 20 and p-ph. 30 show no significant difference to each other in the timing of the process during the seven first days. From day 8, however, worms amputated more anteriorly produce more segments than those amputated in more posterior positions. Statistics for (A) and (D): 2-way ANOVA on repeated measures using Tukey correction were done. In (D), for the sake of simplicity, statistics for the difference between the anterior (p-ph. 3 and 5) and medium (p-ph. 10 and 20) positions are not shown on the graph and are available upon request. * $p < 0.05$; * * $p < 0.01$; * ** $p < 0.001$; * *** * $p < 0.0001$. Error bar: SD.

of the worms (Fig. S1). At 1-day post amputation (1 dpa), the amputation surface is fully covered by a wound epithelium but there is no sign of any outgrowth of tissues (stage 1; Fig. 1B,K), indicating that wound healing is already achieved at this stage. At 2 dpa, a small posterior protuberance (regenerated region) is observed with a depression on its ventral side that probably corresponds to the position of a

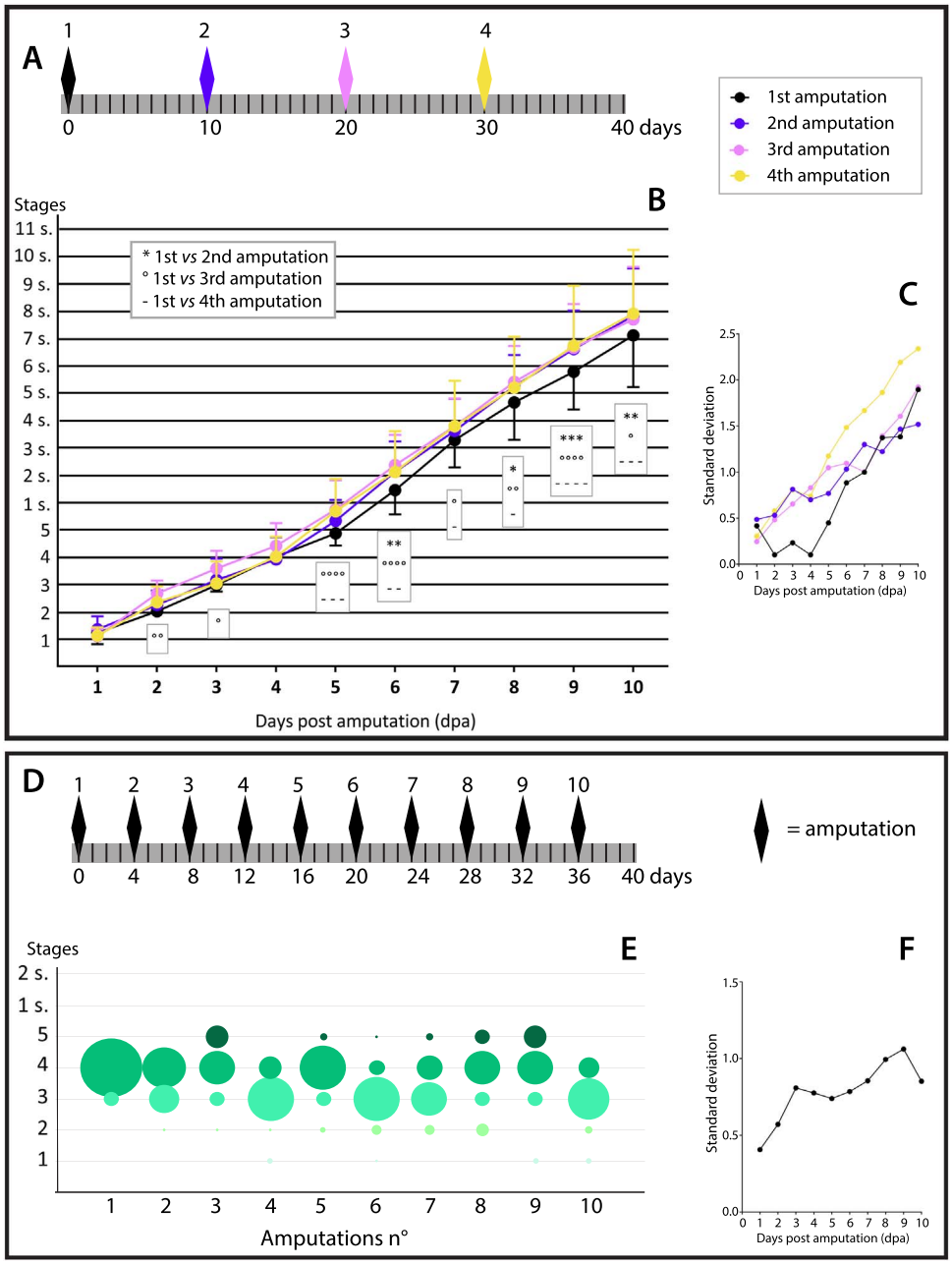

Fig. 3. Posterior regeneration abilities are maintained after multiple amputations. (A) Schematic representation of the experiment with four serial amputations performed every ten days. A time line of 40 days is represented in grey with a black bar for each day. Scoring was done every day. Each amputation is represented by a diamond of a specific color as follows: first amputation in black, second amputation in blue, third amputation in pink and fourth amputation in yellow. The same color code is used in (B) and (C). (B) Graphic representation of the stages reached by the worms every day during ten days after each of the four successive amputations. Efficient regeneration is observed after the four serial amputations and tends to be slightly faster after the second, third and fourth amputations as compared to the first one (n = 24). (C) Graphic representation of the SD (used as a measure of inter-individual variability) of the stages reached by the worms during the ten days following amputation after each of the four successive amputations. Variability tends to increase after the successive amputations and becomes very important after the fourth one. (D) Schematic representation of the experiment with ten serial amputations every four days. Each amputation is represented by a black diamond. Scorings were done just before performing a new amputation. (E) Bubble chart representation of the stages reached by the worms four days after each of the 10 amputations. Bubble diameters are proportional to the number of worms at a specific stage. Color-code of the bubble is that of Fig. S1. Regeneration abilities are maintained after ten serial amputations and there is no clear tendency for either an increase or a decrease of the speed of the process. (n = 30) (F) Graphic representation of the SD of the stages reached by the worms four days after each of the ten successive amputations. Variability tends to increase during the successive amputations. Statistics for (B): 2-way ANOVA on 2 factors repeated measures using Dunnett correction was performed. * $p < 0.05$; * * $p < 0.01$; * ** $p < 0.001$; * *** $p < 0.0001$. Error bar: SD.

reformed anus. A loosely organized gut-like structure can be seen in the regenerated region, but no other differentiated internal structures are found (stage 2; Fig. 1C,H,H',L). At 3 dpa, the regenerated region has clearly increased in size and very small anal cirri are observed. A well-differentiated gut is present (stage 3; Fig. 1D,I,I',M). The size of the regenerated region continues to increase during the two following days. At 4 dpa, a well differentiated pygidium with long anal cirri is present (stage 4; Fig. 1E,N). At 5 dpa, small lateral indentations separate the pygidium from the more anterior part of the regenerated region in which faint segmental grooves start to be seen. The ventral nerve cord and ventral body wall muscles become distinguishable in the regenerated region (stage 5; Fig. 1F,J,J',O). During the following days, segments with conspicuous boundaries and developing parapodia can be seen and their number increases rapidly. Their number however varies among the worms and at 10 dpa ranges from 4 to 11 (Fig. S1).

We conclude that *P. dumerilii* posterior regeneration is a rapid

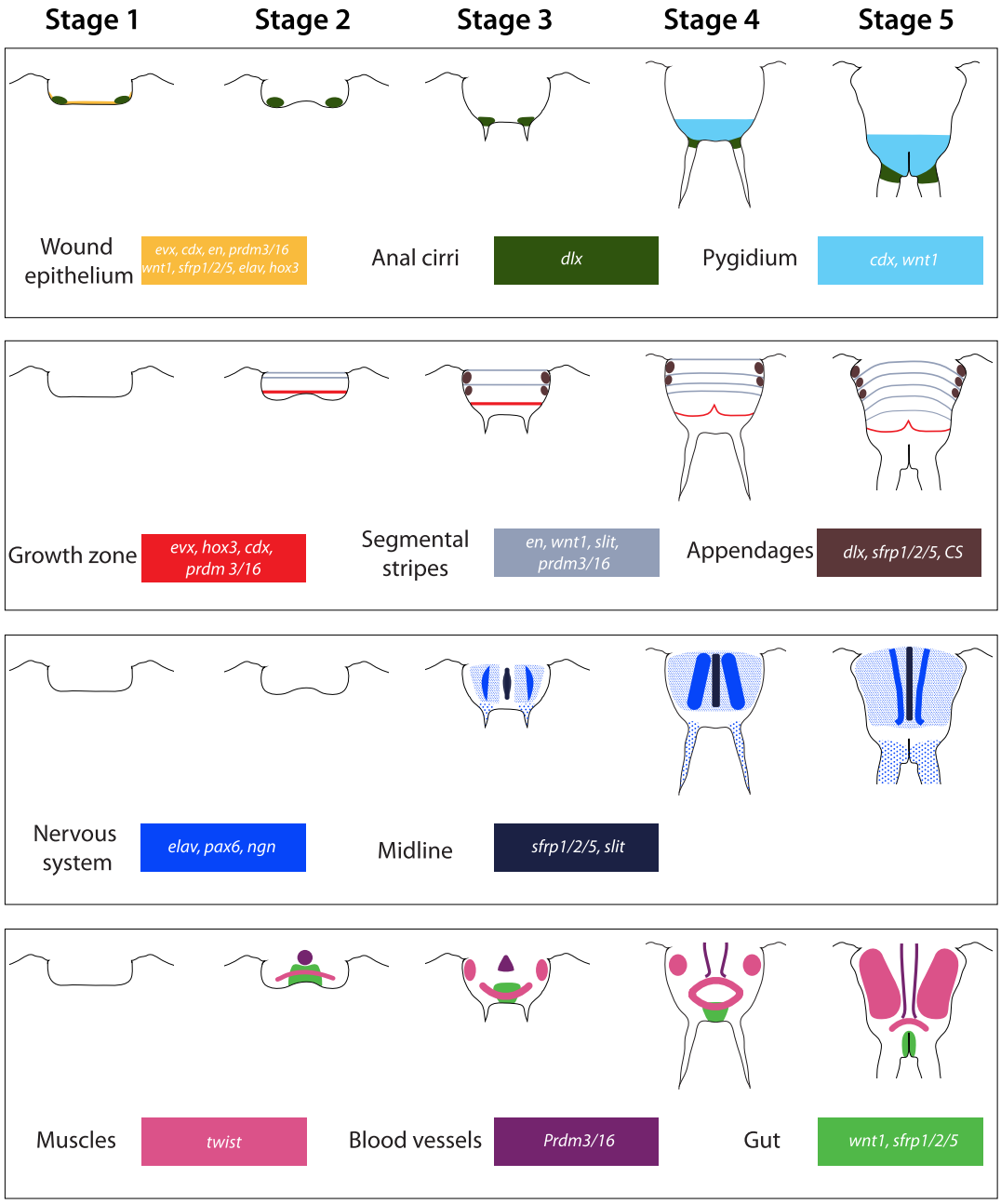

Fig. 4. Summary of the expression during posterior regeneration of the studied genes involved in segment, organ or tissue patterning and differentiation. Schematic drawings of the regenerated region at stages 1 to 5 (ventral views), as well as territories of expression for various organ, structures or tissues, are shown. Each organ, structure or tissue is color-coded and the list of genes expressed therein is mentioned.

process (wound healing is achieved one day after amputation and posterior growth is underway about five days later) which follows a reproducible path and timeline, allowing us to define a precise staging system that will be used for further characterization.

3.2. *Parameters influencing* P. dumerilii *posterior regeneration*

We studied parameters that may affect posterior regeneration efficiency and timing. For all these experiments, the worms were 'scored' at different time points after amputation by defining the regeneration stage that they had reached (stages 1 to 5) for early time points, or, for later time points, the number of morphologically well-distinguishable segments that have been produced. We first tested the influence of worm 'size' (number of segments) by comparing regeneration of worms with three different segment number ranges, 10–20 segments ('small worms'), 30–40 segments ('intermediate worms', previously used to define the regeneration stages) and 70–80 segments ('big worms'; Fig. 2A). Efficient regeneration with the aforementioned reproducible stages was observed in the three categories of worms. While the timing of the process was similar in intermediate and big worms, regeneration of small worms was significantly accelerated at 1 dpa. This timing difference was kept during all following days, resulting in the production of significantly more segments than for intermediate and big worms at 10 dpa (Fig. 2A). Interindividual variability differed in the three worm categories and was the lowest in the 30–40 segment worms (Fig. 2B) that were therefore used for all next experiments.

We next assessed the influence of the position of the amputation site, by comparing seven different ones as shown in Fig. 2C (post-pharynx (p-ph.) segment 30 corresponds to the amputation site used in the previous experiments). Worms amputated at p-ph. segment 0 (immediately posterior to the pharynx) died within one or two days without any sign of regeneration and showed an eversion of the pharynx through the amputation site, which could be the cause of death (n = 12, not shown). Similarly, all but one worm (n = 12) amputated at p-ph. segment 1 presented an eversion of the pharynx and died (not shown). Worms amputated at p-ph. segment 3, 5, 10, 20 or 30 were able to regenerate but with some timing differences. Worms amputated at p-ph. segment 3 or 5 showed a significantly delayed regeneration from 3 dpa, which resulted in a delayed production of segments in worms amputated at p-ph. segment 3 (Fig. 2D). In addition, the rate of segment addition differed in worms amputated at p-ph. segment 10, 20 or 30 and is significantly higher if the position of the amputation is more anterior (Fig. 2D).

We finally tested how regeneration is impacted by repeated amputations. In a first experiment, we performed four serial amputations with intervals of ten days (at that time the worms have already regenerated the pygidium and produced several segments) and scored the worms every day during the whole experiment (Fig. 3A). Regeneration ability was maintained during these four occurrences of regeneration with only minor modifications of its timing (Fig. 3B). However, interindividual variability became however high after the fourth amputation (Fig. 3C). Next, we performed ten serial amputations with intervals of only four days, meaning that new amputations were made before the worms resumed their segment production, and we scored the worms every four days just before making new amputations (Fig. 3D). We found that most worms normally regenerate after all serial amputations (Fig. 3E). There was no clear tendency for either an increase or a decrease of the speed of the process. However, interindividual variability tended to increase (Fig. 3F) and a small number of worms showed abnormally shaped pygidium and anal cirri after several amputations (not shown).

We therefore conclude that *P. dumerilii* posterior regeneration is only influenced in a minor manner by worm size. Regenerative abilities are not specific of the posteriormost segments, as efficient regeneration is observed when amputations are made at different positions along the animal body axis. However, amputations very close to the pharynx induce its eversion through the wound and early mortality of the worms, which precludes these worms from being able to regenerate. Regenerative abilities persist upon repeated amputations without important alterations of the process, even after ten successive and closely repeated amputations.

3.3. Molecular and cellular characterization of P. dumerilii posterior regeneration

To further characterize *P. dumerilii* posterior regeneration, we performed whole-mount *in situ* hybridizations (WMISH) for 14 genes previously shown to be involved in segment, organ or tissue patterning and differentiation in *P. dumerilii* (Table S1; Fig. 4). Expression of these genes were previously established during posterior elongation in about one-year-old worms (10–12 days post amputation when many segments have been produced; Gazave et al., 2013). We found very similar expressions in 30–40 segment (3–4-month-old) worms at 5 dpa (stage 5; Fig. S2). Fig. 5 shows representative images (ventral views) of the expression of all the genes at earlier stages (stage 1–4). Additional images (mainly dorsal views) highlighting other interesting aspects of their expression are shown in Fig. S3. Hereafter, we provide a detailed characterization of these expressions, which are summarized and schematically represented in Fig. 4, highlighting how these gene expressions provide important information about the timing of *P. dumerilii* posterior regeneration.

We first studied the expression of three genes known to be expressed in the growth zone and the pygidium (*Pdum-hox3*, *Pdum-evx* and *Pdum-cdx*; Figs. 4, 5A-C'", Fig. S2A-F; de Rosa et al., 2005; Gazave et al., 2013). These genes are expressed at stage 1 in the posteriormost cells of the body, including the wound epithelium (Figs. 4, 5A,B,C, red arrows). Their expression domains slightly extend at stage 2 (Fig. 5A',B',C') and from stage 3 become very similar to those found at stage 5 (Fig. S2A-F), with a sharp expression of *Pdum-hox3* and *Pdum-evx* in a ring of cells corresponding to the growth zone and a broader expression of *Pdum-cdx* in both the growth zone and pygidium (Figs. 4, 5A"-C'", Fig. S3A-C, red arrowheads and blue arrows, respectively). These expression patterns are therefore suggestive of an early regeneration of the growth zone, as early as stage 3.

We next monitored segment formation and, for that purpose, we studied the expression of *Pdum-engrailed* (*Pdum-en*) and *Pdum-wnt1* (Prud'homme et al., 2003), which are expressed during early or late phases of segment formation, respectively (Fig. 5D-E'", Fig. S2G,H). *Pdum-wnt1* is also strongly expressed in the posterior-most part of the gut and in the pygidial epidermis (Fig. 5E'-E'", Fig. S2H,I, green and blue arrows, respectively; Janssen et al., 2010). Both genes are expressed at stage 1 in the wound epithelium (Figs. 4, 5D,E, red arrows). From stage 2 to stage 4, *Pdum-en* is strongly expressed in a stripe of cells at the border between the last non-amputated segment and the regenerated region, as well as in stripes of ectodermal cells in the regenerated region (Figs. 4, 5D'-D'", blue asterisks and arrowheads, respectively). From stage 2, *Pdu-wnt1* is expressed in the posterior-most part of the gut and, from stage 3, also in peripheral posterior cells, probably pygidial epidermal cells (Fig. 5E'-E'", green and blue arrows, respectively). In addition, at stage 4, one or two faint ectodermal stripes of *Pdum-wnt1* expression can be observed on the dorsal side of the regenerating part (Fig. S3D, blue arrowheads). At stage 5, additional stripes of *Pdum-en* and *Pdum-wnt1* expression are present (Fig. S2G,H, blue arrowheads). We conclude that segment formation starts very early during regeneration: a first segment could be specified at stage 2 and additional segments are added from stage 3–5, suggesting the presence of an already active growth zone from early stages of regeneration.

One conspicuous feature of *P. dumerilii* segments is the presence of appendages (parapodia). An early marker of appendage formation is *Pdum-dlx* which is expressed in the primordia of parapodia and cirri (Grimmel et al., 2016). At stage 1 and 2, *Pdum-dlx* is expressed in two bilateral patches of cells that correspond to the position where the anal cirri will form (Figs. 4, 5F-F', brown arrows) and, at later stages, in a large group of cells at the basis of the developing anal cirri (Fig. 5F"-F'", brown arrows). At stage 3, we also observed two small bilateral groups of *Pdum-dlx*-expressing cells more anteriorly, which likely correspond to the anlagen of the parapodia of two developing segments (Fig. 5F", brown arrowheads). Developing parapodia with a large number of *Pdum-dlx*-expressing cells are observed at stage 4 and 5 (Figs. 4, 5F", Fig. S2J, brown arrowheads). We also analysed the expression of *Pdum-sfrp1/2/5*, a putative secreted antagonist of Wnt signaling (Bastin et al., 2015). At stage 1, this gene is strongly expressed in the wound epithelium (Figs. 4, 5G, red arrows). At stage 2, this expression fades away and strong expression is found in the gut (Figs. 4, 5G', green arrows, Fig. S3F), the dorsal epidermis and the posterior part of the parapodia of the differentiated segment that abuts the amputation site (Fig. 5G', brown asterisks, Fig. S3F). At stage 3, the two latter sites of expression are still observed (Figs. 4, 5G", Fig. S3F'). At stage 4 and 5, *Pdum-sfrp1/2/5* is expressed in cells of the developing parapodia (Figs. 4, 5G'", Fig. S2K, brown arrowheads), epidermal cells (in particular on the dorsal side, Fig. 5G'", Figs. S2L, S3F", blue arrowheads) and ventral midline cells (Fig. 5G'", Fig. S2K, black arrowhead). A late step of parapodia development is the formation of chaetae, the characteristic chitinous bristle of annelid appendages, whose early formation is marked by the expression of Chitin Synthase (CS)-encoding genes such as *Pdum-cs1* (Gazave et al., 2017; Zakrzewski et al., 2014). Expression of this gene is found only in the most anterior segment of the regenerated region at stage 4 and 5

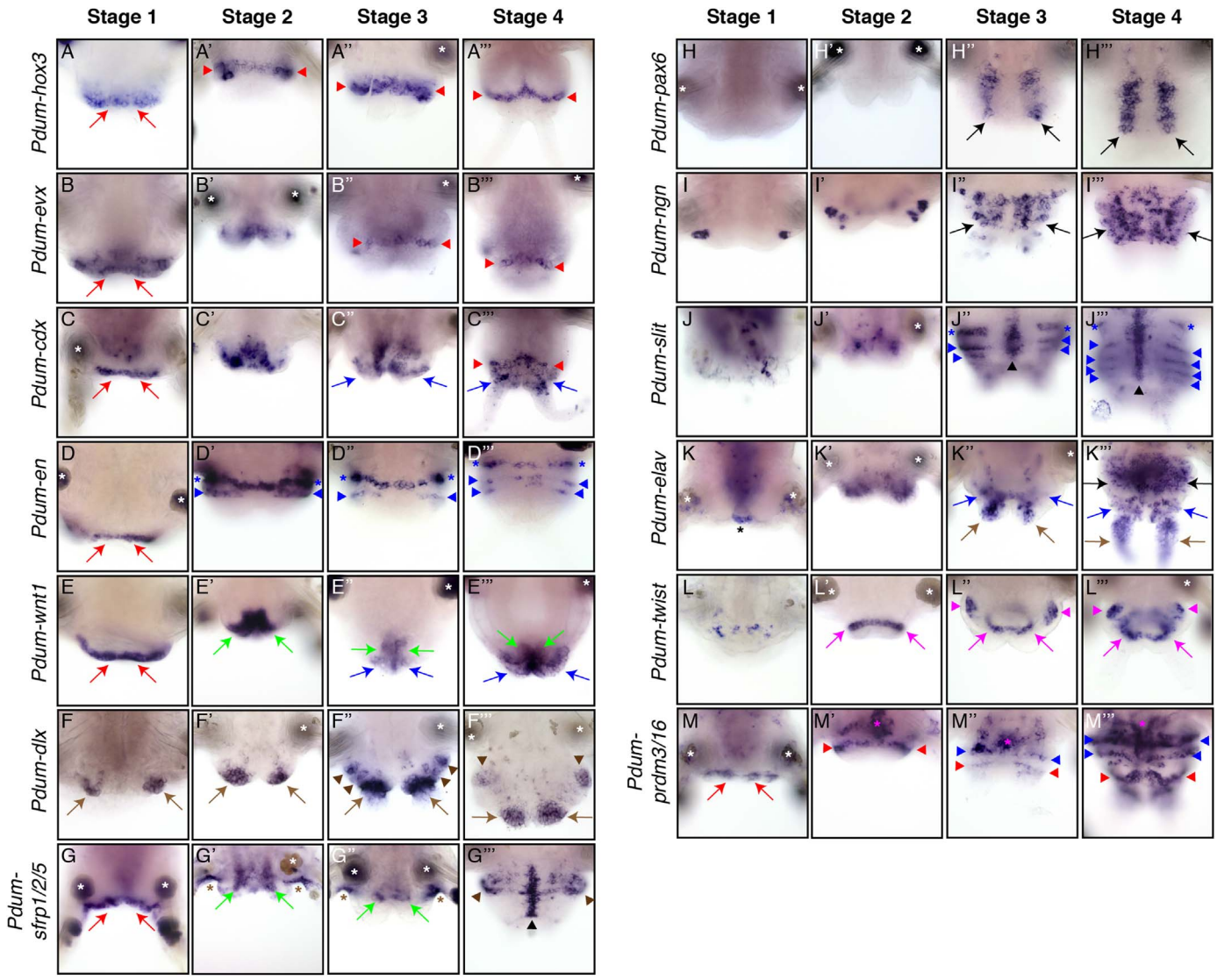

Fig. 5. Expression during posterior regeneration of genes involved in segment, organ or tissue patterning and differentiation. WMISH for the genes whose name is indicated are shown for four posterior regeneration stages (stage 1 to 4). Stage 5 WMISH images are shown in Fig. S2. All panels are ventral views (anterior is up). Red arrows = wound epithelium; brown arrows = anal cirri; green arrows = intestine; blue arrows = pygidium; black arrows = neurectoderm or ventral nerve cord; pink arrows = pygidial muscles; red arrowheads = posterior growth zone; blue arrowheads = segmental stripes; brown arrowheads = parapodia; black arrowheads = ventral midline; pink arrowheads = segmental muscles; blue asterisks = expression in cells at the border between last non-amputated segment and regenerated region; brown asterisks = expression in the last non-amputated segment; pink asterisk = blood vessels; black asterisk = early expression in the ventral part of the wound epithelium, abutting the ventral nerve cord. White asterisks indicate non-specific staining of secreting glands associated to parapodia.

(Figs. S2M, S3E, yellow arrowhead). Taken together, these expression data suggest that parapodial anlagen are specified as early as at stage 3 and that developing parapodia are present from stage 4.

We next focused on nervous system formation during regeneration. Prior work has shown that ventral nerve cord (VNC) formation during *P. dumerilii* larval and post-larval development involves the successive expressions of several genes, such as *Pdum-pax6* early expressed in the ventro-lateral part of the trunk ectoderm, *Pdum-neurogenin* (*Pdum-ngn*) expressed a bit later in most or all neural progenitors, *Pdum-slit* expressed in ventral midline cells, and *Pdum-elav* whose expression is found in most or all differentiating neurons (Figs. 4, 5 H-K”’, Fig. S2N-Q; Denes et al., 2007; Simionato et al., 2008; Béhague, Kerner, Balavoine and Vervoort, unpublished observations). *Pdum-pax6* is expressed from stage 3–5 in two longitudinal ventro-lateral bands of cells in the anterior part of the regenerated region, which likely correspond to neurectodermal domains of the future segments (Figs. 4, 5H-H”’, Fig. S2N, black arrows). No expression is observed at earlier stages (Fig. 5H-H’). *Pdum-ngn* is expressed at stage 1 and 2 in a few lateral cells of unknown identity (Fig. 5I-I’). From stage 3, it starts to be expressed in many cells on the ventral side of the regenerated region, probably neural progenitors of both the VNC and the peripheral nervous system of the developing segments, as well as in some cells of the pygidium, in particular cells associated to the anal cirri (Figs. 4, 5I”-I”’, Fig. S2O, black and brown arrows, respectively). *Pdum-slit* is first expressed in a few scattered cells at stage 1 and 2, and from stage 3 in ventral midline cells, as well as in ectodermal segmental stripes (Figs. 4, 5J-J”’, Fig. S2P, black and blue arrowheads, respectively). *Pdum-elav* is expressed at stage 1 in cells of the ventralmost part of the wound epithelium, close to the amputated VNC (Figs. 4, 5K, black asterisk). At stage 2, *Pdum-elav* is expressed in many cells in the ventral part of the regenerated region (Fig. 5K’). From stage 3, its expression is observed in many cells, likely differentiating neurons of developing segments, pygidium and anal cirri (Fig. 5K”,K”’, Fig. S2Q, black, blue and brown arrows, respectively). To further characterize nervous system regeneration, we performed immunolabelings with antibodies against acetylated tubulin during regeneration

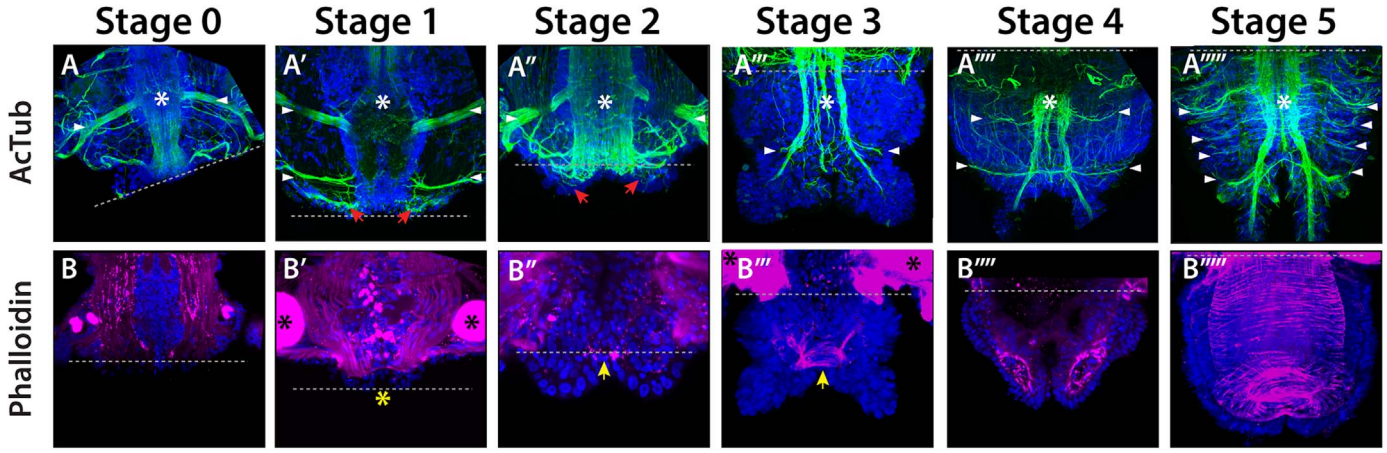

Fig. 6. Nervous system and muscle differentiation during posterior regeneration. All pictures are ventral views (anterior is up) of posterior part of worms counterstained with Hoechst nuclear staining (in blue). Maximum projections of all Z-sections that represent about 2/3 of the posterior region's thickness are shown. (A-A⁗′) Antibodies against acetylated tubulin (green) label the axon scaffold of the ventral nerve cord (VNC, white asterisk) and peripheral nerves (white arrowheads). Stage 0 corresponds to worms that have been fixed immediately after amputation. At stages 1 and 2, bilateral nerves underlying the wound epithelium are observed (red arrows). From stage 3 onwards, peripheral nerves are observed in the regenerated region, some of which extending from the VNC into the anal cirri. (B-B⁗′) Phalloidin labeling (purple) allows the visualization of differentiated muscle fibers. At stage 0 (B), muscle fibers are sharp cut. One day later (stage 1, B'), muscle fibers are contracted close to the amputation site (yellow asterisk) and, at stage 2, pygidial muscles start to differentiate (B″, yellow arrow). Later on (stage 3 to 5), segmental and gut-associated muscles progressively differentiate (B‴-B⁗′). Black asterisks indicate non-specific staining of secreting glands associated to parapodia. Grey dotted lines indicate the amputation site.

(Fig. 6A-A⁗′). We observed at stage 1 and 2 the presence of bilateral nerves that extend from the ventral towards the dorsal side of the worms and that underlie the wound epithelium (Fig. 6A',A", red arrows). From stage 3 onward, a well-differentiated VNC is present in the regenerating region (white asterisk), which progressively becomes more complex and produces peripheral nerves (Fig. 6A‴-A⁗′, white arrowheads). To better understand when the bilateral nerves observed at stage 1 start to develop, we performed immunolabelings at different time points between amputation time and 1 dpa. These nerves, which are not distinguishable in worms immediately after amputation (0 dpa; Fig. 6A), are present as early as five hours post amputation (5hpa; Fig. S4A-A‴, red arrows). Whether these nerves correspond to new nerves extending from the VNC or to modifications of existing peripheral nerves cannot be ascertained. Taken together, these data indicate that nervous system formation in the regenerated part has already started at stage 3 and follows similar steps as compared to its initial formation during development and growth.

We also studied the formation during regeneration of mesodermal derivatives, namely somatic muscles and blood vessels. We used the expression of *Pdum-twist* as marker of somatic muscle development (Pfeifer et al., 2013), as it is expressed in the developing segmental and pygidial muscles (Fig. 4, Fig. S2R, pink arrowheads and arrows, respectively). At stage 1, a weak expression is observed in a few cells (Fig. 5L). From stage 2, *Pdum-twist* is strongly expressed in a ring of internal cells (Figs. 4, 5L'-L‴, pink arrows), probably mesodermal cells that will produce the pygidial circular muscles. In addition, from stage 3, two bilateral and more anterior groups of *Pdum-twist*-expressing cells are detected (Figs. 4, 5L",L‴, Fig. S2R, pink arrowheads), which correspond to the developing somatic segmental mesoderm. To further analyze muscle formation, we performed phalloidin labelings during regeneration, which suggest that differentiation of pygidial muscles starts at stage 2 and that of segmental muscles at stage 4 (Fig. 6B-B⁗′). We also studied the expression of *Pdum-prdm3/16* (Vervoort et al., 2016; Kerner and Vervoort, unpublished observations). At stage 1, this gene is expressed in the wound epithelium (Figs. 4, 5M, red arrows). At stage 2 and 3, *Pdum-prdm3/16* expression is found in dorsal and ventral medial patches of cells that might correspond to precursor cells of the blood vessels (Fig. 5M',M", Figs. S3G,G', pink asterisk), as well as in the growth zone (Fig. 5M',M", red arrowheads) and developing segments (Fig. 5M',M", blue arrowheads). These latter expression sites are also observed at later stages, in addition to a strong expression in both ventral and dorsal blood vessels (Fig. 5M",M‴, Figs. S2S-T, S3G", pink asterisk). Taken together, these expression data suggest that the specification of mesodermal structures starts as early as at stage 2.

In conclusion, our gene expression study indicates that *P. dumerilii* posterior regeneration is a very fast process (Fig. 4): at stage 3, a functional growth zone is present and has already produced segments in which neurogenesis and mesodermal structures formation are ongoing, and the pygidium has already undergone its differentiation. Some tissue specification, in particular mesodermal tissues, occurs even earlier, at stage 2, and parapodia development starts at stage 3.

3.4. *Stem cell gene expression during* P. dumerilii *posterior regeneration*

We previously showed that homologs of several genes known to be expressed in other animals in somatic and/or germinal stem cells (hereafter named 'stem cell genes') were expressed in the posterior growth zone in *P. dumerilii* (Gazave et al., 2013). The posterior growth zone contains two subpopulations of putative stem cells, one superficial (probably ectodermal) and the other internal (probably mesodermal), which express different combinations of stem cell genes and are located on the ventral and dorsal side of worms, respectively (Gazave et al., 2013). Most of these genes are expressed not only in the growth zone cells, but also in a graded manner in mesodermal and/or ectodermal cells of developing segments (Gazave et al., 2013). In the present work, we studied the expression of some of these genes during regeneration. This includes a previously characterized *piwi* gene (Rebscher et al., 2007). Using available transcriptomic data (Chou et al., 2018), we identified and cloned a second *P. dumerilii piwi* homolog – the previously known gene and the newly discovered one were named *Pdum-piwiA* and *Pdum-piwiB*, respectively, based on phylogenetic analysis (Fig. S5). Expression patterns of all the selected stem cell genes at stage 5 are shown in Fig. S6. These expressions are similar to those previously reported, with a few differences, as we did not detect *Pdum-piwiA* and *Pdum-vasa* expression in the ectodermal part of the growth zone, in contrast to what was previously observed in older worms 12 days after amputation (Gazave et al., 2013).

The expression patterns of all selected stem cell genes at stages 1–4 of regeneration are shown in Fig. 7. At stage 1, *Pdum-piwiA* and *Pdum-piwiB* genes are expressed in the differentiated segment adjacent to the amputation site, in very few isolated cells and two bilateral patches of

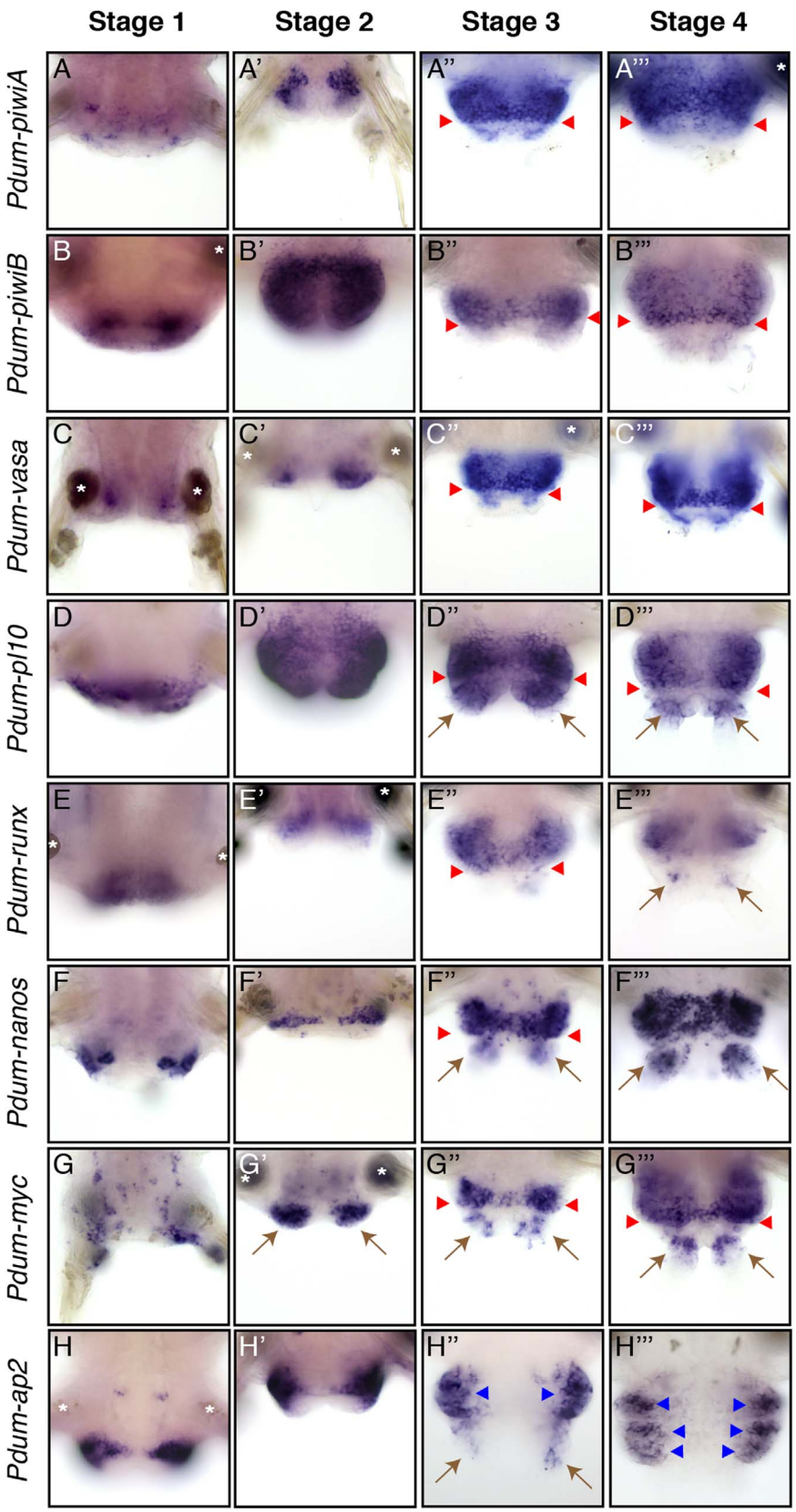

Fig. 7. Expression of 'stem cells genes' during posterior regeneration. WMISH for the genes whose name is indicated are shown for four posterior regeneration stages (stage 1 to 4). Stage 5 WMISH images are shown in Fig. S6. All panels are ventral views (anterior is up). Brown arrows = anal cirri; red arrowheads = posterior growth zone; blue arrowheads = segmental stripes. White asterisks indicate non-specific staining of secreting glands associated to parapodia.

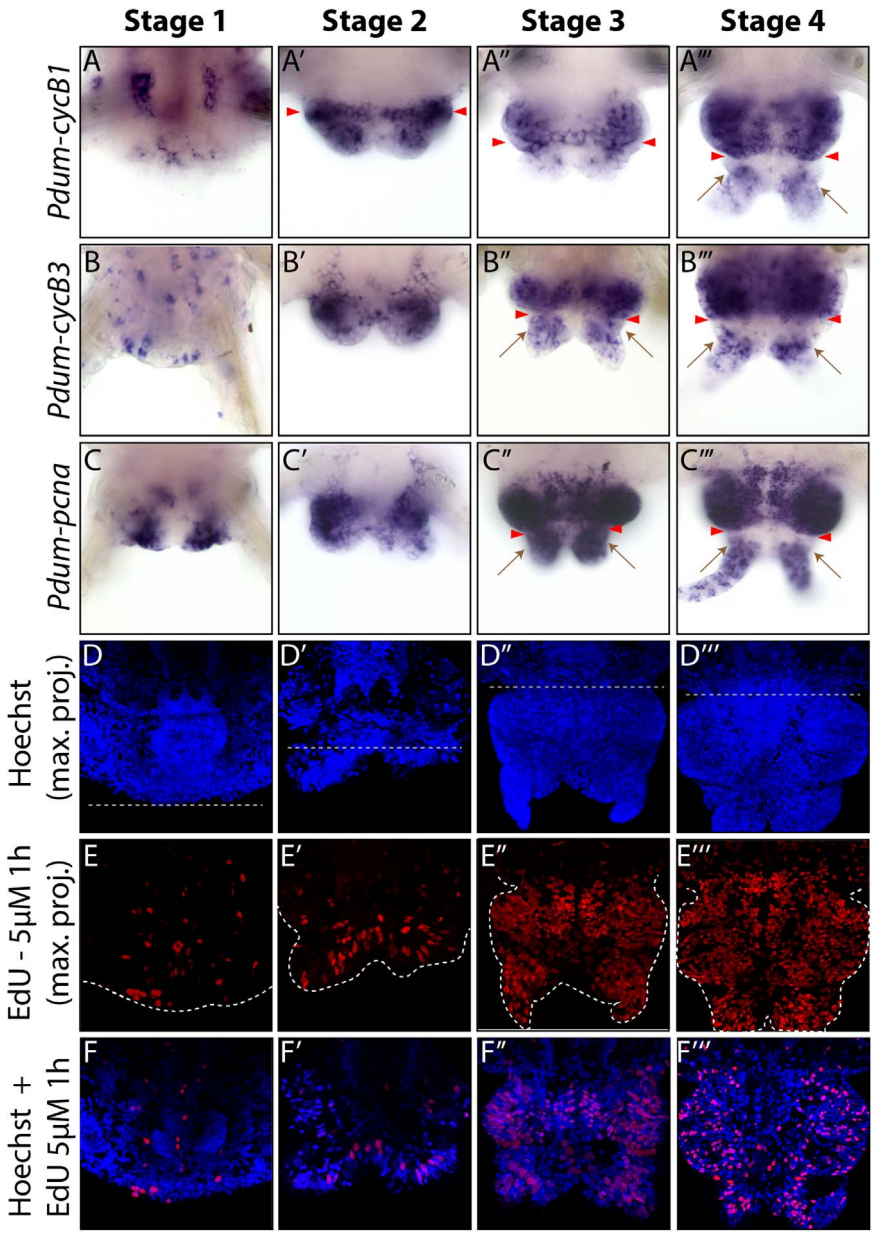

Fig. 8. Cell proliferation during posterior regeneration. (A-C"') WMISH for three cell cycle genes (*Pdum-cycB1*, *Pdum-cycB3* and *Pdum-pcna*) are shown for four posterior regeneration stages (stage 1 to stage 4). All images are ventral views, anterior is up. Red arrowheads = posterior growth zone; brown arrows = anal cirri. (D-F"') Posterior parts of worms (anterior is up) showing Hoechst nuclear staining (blue) and/or EdU labeling (red) for four posterior regeneration stages (stage 1 to stage 4) after one hour of EdU incorporation (5 µM). D to E"' are maximum projections (max. proj.) of all Z-sections. In E to E"', white dotted lines show the delineation of the observed specimens as defined by Hoechst staining. F to F"' are projections of a subset of the Z-sections, which allow to realize that, even in stage 3 and 4, only a fraction of the nuclei is EdU+ . Grey dotted lines indicate the amputation site.

cells, respectively (Fig. 7A,B). No clear expression of *Pdum-vasa* can be detected at this stage, while *Pdum-pl10* is expressed in many cells of the posterior part of the differentiated segment (Fig. 7C,D). At stage 2, *Pdum-piwiA* and *Pdum-vasa* are expressed in bilateral groups of internal cells in the regenerated region (Fig. 7A',C'). *Pdum-piwiB* and *Pdum-pl10* are expressed in most cells of this region (Fig. 7B',D'), the latter being also expressed in superficial cells on the ventral side (not shown). The two *P. dumerilii piwi* genes therefore show clearly distinct expression patterns during early stages of regeneration. From stage 3, the four genes are expressed in the mesodermal growth zone and mesoderm of the developing segments (Fig. 7A"-D"', red arrowheads). *Pdum-pl10* is in addition strongly expressed in cells at the basis of the anal cirri (Fig. 7D"-D"', brown arrows) and in the ectodermal part of the growth zone (Fig. S3H, red arrowheads). At stage 5, *Pdum-piwiA*, *Pdum-piwiB*, *Pdum-vasa*, and *Pdum-pl10* are expressed in the mesodermal part of the growth zone (Fig. S6A-D, red arrowheads), mesodermal cells of the developing segments, and more or less strongly in cells at the basis of the anal cirri (Fig. S6A-D, brown arrows).

At stage 1, *Pdum-runx* is weakly expressed in the ventral posteriormost part of the last differentiated segment (Fig. 7E). Weak expression in internal cells in the regenerated region is observed at stage 2 (Fig. 7E'). At stage 3, it is expressed in the mesodermal growth zone and the developing mesoderm (Fig. 7E", red arrowheads). The expression in the growth zone fades away at stage 4 and a weak expression in the anal cirri can be observed (Fig. 7E"', brown arrows). At stage 5, *Pdum-runx* is weakly expressed in the developing mesoderm (Fig. S6E). We did not detect clear expression in the mesodermal growth zone in contrast to what has been reported in older worms (Gazave et al., 2013). *Pdum-nanos* is expressed in two lateral patches of superficial cells in the differentiated segment close to the amputation at stage 1 (Fig. 7F). At stage 2, its expression extends ventrally at the border between the differentiated segment and the regenerated region

(Fig. 7F'). At stage 3 and 4, *Pdum-nanos* expression is similar to that seen at stage 5 (Fig. S6F), with strong expression in the ectodermal growth zone (Fig. 7F"-F"', red arrowheads), developing nervous system and anal cirri (Fig. 7F"-F"', brown arrows). At stage 1, *Pdum-myc* is expressed in many scattered cells in the last differentiated segment (Fig. 7G). Strong expression of the gene is observed at stage 2 in two posterior patches of cells located where the anal cirri will form (Fig. 7G', brown arrows). At stage 3 and 4, *Pdum-myc* is expressed in both ectodermal and mesodermal parts of the growth zone (Fig. 7G",G"', Fig. S3I, red arrowheads), developing segments and anal cirri (Fig. 7G",G"', Fig. S3I, brown arrows). Expression is detected at stage 5 in the mesodermal and ectodermal parts of the growth zone (Fig. S6G, red arrowheads), in the developing segmental mesoderm and ectoderm, and in anal cirri (Fig. S6G, brown arrows). At stage 1, *Pdum-ap2* is strongly expressed in two dorso-lateral patches of cells on the ventral side of the last differentiated segment (Fig. 7H) and in the dorsal part of the wound epithelium (Fig. S3J). Strong dorso-lateral and dorsal expression can also be observed at later stages and additional expression in the developing anal cirri is also observed (Fig. 7H'-H"', Fig. S3J'-J"', blue arrowheads, red arrowheads and brown arrows, respectively). At stage 5, *Pdum-ap2* is expressed in dorso-lateral stripes of epidermal cells (Fig. S6H, blue asterisks and arrowheads) and in the ectodermal part of the growth zone (Fig. S6I, red arrowheads).

All the studied stem cell genes are therefore expressed during *P. dumerilii* posterior regeneration and several of them are broadly expressed during early stages of the process (stage 2 and even stage 1 for some genes). As these genes are usually expressed in proliferating cells in other models and during *P. dumerilii* growth (Gazave et al., 2013), we next studied cell proliferation at different stages of regeneration.

3.5. Cell proliferation during P. dumerilii posterior regeneration

As a first approach to identify proliferating cells, we studied the expression of three previously characterized cell cycle genes, *Pdum-cycB1*, *Pdum-cycB3* and *Pdum-pcna* (Demilly et al., 2013; Gazave et al., 2013). *Pdum-cycB1* and *Pdum-cycB3* have similar expression patterns throughout the regeneration process (Fig. 8A-B"', Fig. S6J,K). At stage 1, the two genes are expressed in a few cells located close to the wound epidermis (Fig. 8A,B). At stage 2, expression is detected in many cells of the regenerated region (Fig. 8A',B'). Broad expression is also observed at stage 3, 4 and 5 in the mesodermal part of the growth zone, the future mesoderm of the developing segments and at the basis of the anal cirri (Fig. 8A",A"',B",B"', Fig. S6J,K, red arrowheads and brown arrows). At stage 1, *Pdum-pcna* is strongly expressed in two large lateral patches of cells at the amputation site, which include cells of the wound epithelium (Fig. 8C). At later stages, *Pdum-pcna* expression is similar to that of the two *cyclin* genes, while being stronger and probably concerning more cells than the other cell cycle genes (Fig. 8C'-C"', Fig. S6L). In addition, strong expression of *Pdum-pcna* is observed in the ectoderm, including the ectodermal part of the growth zone (Fig. S3K-K", Fig. S6M), in contrast with *Pdum-cycB1* and *Pdum-cycB3*.

To confirm the cell proliferation patterns that can be deduced from cell cycle gene expressions, we performed EdU incorporations which allow labeling cells that are in S phase. We incorporated EdU for one hour at different stages of regeneration, followed by immediate fixation (Fig. 8D-F"', the EdU profile of stage 5 is not shown, as it is identical to the previously published one during posterior elongation; Gazave et al., 2013). At stage 1, few EdU+ cells are found in the segment adjacent to the amputation site (Fig. 8D,E,F). Similar distributions of labeled cells were observed when EdU was incorporated immediately before or after amputation (Fig. S7), suggesting that there is no major impact of amputation on cell proliferation until stage 1. At stage 2, EdU+ cells are found in both the regenerated region and adjacent segment (Fig. 8D',E',F'). At stage 3 to 5, much more labeled cells are detected in the regenerated part, in both its anterior part that will give rise to segments and the developing anal cirri (Fig. 8D"-D"',E"-E"',F"-F"').

The expression of cell cycle genes and the distribution of EdU+ cells therefore point out strong cell proliferation during most stages of regeneration, raising the possibility that it may be required for regeneration to proceed in a normal way. To test this hypothesis, we treated worms with widely-used anti-proliferative agents, hydroxyurea (HU) and nocodazole, and analysed their effects on regeneration. While completely blocking regeneration, nocodazole was highly toxic, even at low concentration (0.01 μM), and caused death of most worms during treatment (not shown), precluding us from drawing from these experiments firm conclusions about the role of cell proliferation during regeneration. HU in contrast appeared to be more harmless to worms: in a first concentration range test experiment, we put worms immediately after amputation in three different HU concentrations (10 mM, 20 mM and 50 mM) for five days and scored the worms every day for the stage that has been reached (Fig. 9A). No worm death was observed and, with the three concentrations used, regeneration was much delayed as compared to controls: at 5 dpa, while control worms were at stage 5, worms treated with HU were mostly at stage 2 and no stage 4 or 5 was observed. While HU-treated worms reached stage 1 at 1 dpa like controls, significant regeneration delays started to be detected at 2 dpa for the 50 mM HU condition. At 5 dpa, worms treated with 50 mM HU tended to regress to previous stages, which could reflect toxic effects of HU at this concentration. We therefore chose 20 mM concentration for further experiments as in this condition putative toxic effects were low or absent. In addition, worms treated with this concentration present less variability in the stage that has been reached than the worms treated with the lowest concentration (Fig. 9A).

To confirm that HU did indeed block cell proliferation in our experiments, we did an EdU pulse and chase experiment: one-hour EdU incorporation was performed at 3 dpa to label cells in S phase and followed by a two-day chase either in sea water (control) or sea water with 20 mM HU (Fig. 9B). As expected, in control worms, many EdU+ positive nuclei were observed (Fig. 9B1) and many of them showed stippled EdU labelings (*i.e.*, non-homogenous labeling of the nucleus), due to EdU dilution during cell divisions having occurred since incorporation (Fig. 9B1'; *e.g.*, Demilly et al., 2013). In contrast, in HU treated worms, a reduced number of labeled nuclei were observed (Fig. 9B2) and all nuclei showed a strong and homogenous labeling, strongly suggesting that these cells did not divide in the presence of HU (Fig. 9B2'). To better understand how regeneration proceeds in presence of HU, we did HU treatment from 0 dpa to 5 dpa, fixed the treated worms at 5 dpa and performed WMISH for some of the genes whose expression was studied during normal regeneration (Fig. S8). All the analysed genes showed expressions at 5 dpa in HU treated worms similar to those of stage 2 in non-treated worms, further indicating that regeneration is blocked in presence of HU and that proliferation is required to reach stage 3.

In order to assess at which stages of regeneration cell proliferation is required, we next performed HU treatment starting at different time points after amputation (from 0 dpa to 5 dpa) and pursued treatment until 10 dpa, scoring the stages reached by worms at 5 dpa, 7 dpa and 10 dpa (Fig. 9C). Worms treated from 0 and 1 dpa reached stage 2 but did not progress beyond this stage. Worms treated from 2 dpa were between stage 3 and 4 at 5 dpa and 7 dpa, but their regenerated region subsequently tended to regress, so at 10 dpa most of these worms present a stage 2 morphology. Treatment from 3 dpa did not allow the worms to go beyond stage 4 and some morphological regressions were also observed in these worms after day seven. Worms treated from 4 and 5 dpa were able to reach stage 5 at 5 dpa, as the control group, but subsequent addition of segments was severely impaired (Fig. 9C). Cell proliferation is therefore required to reach stage 3 and for further progression of regeneration and segment addition. We also tested if HU treatment was reversible by starting HU treatment immediately after

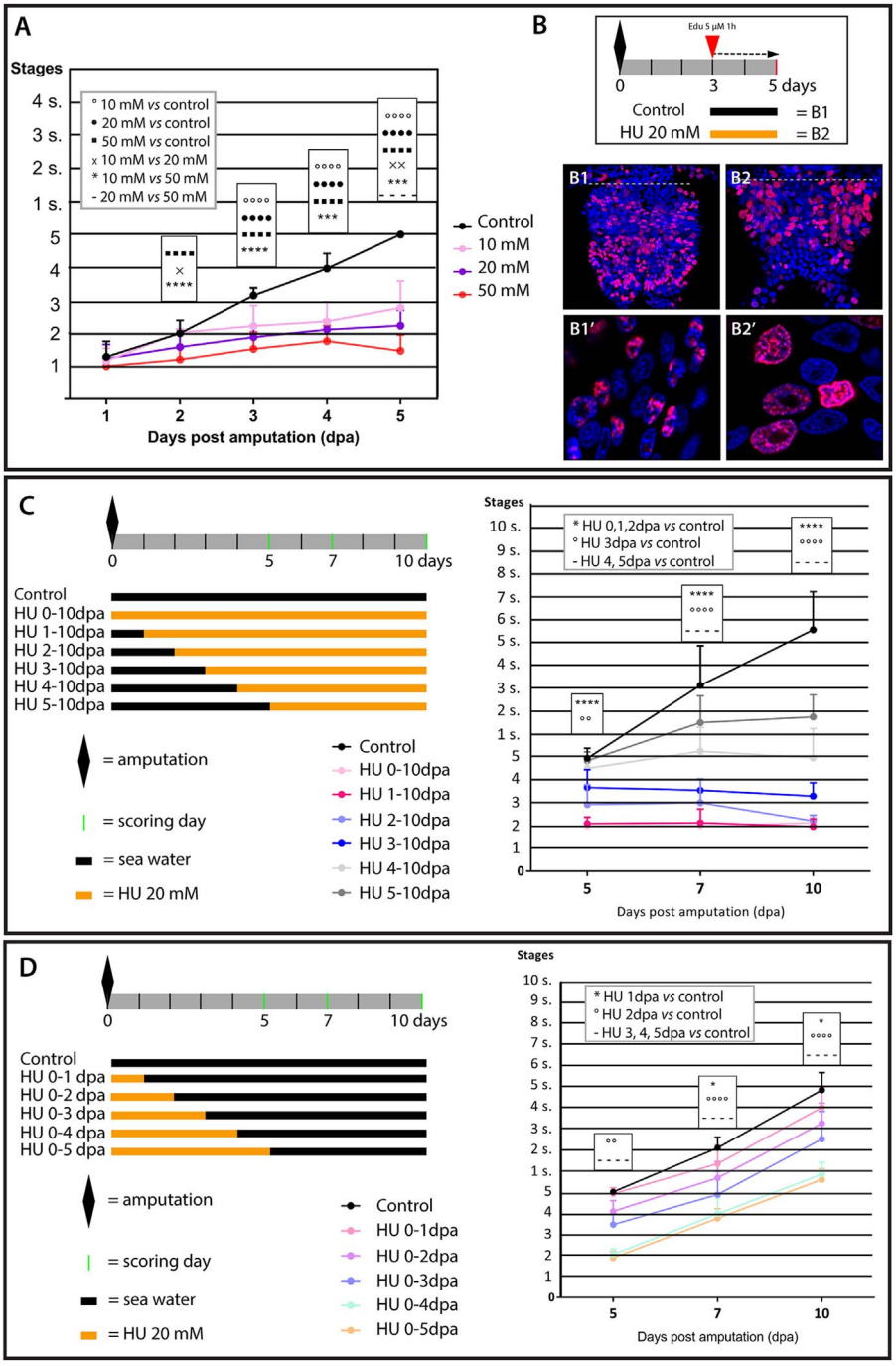

Fig. 9. The anti-proliferative agent hydroxyurea (HU) impairs posterior regeneration in a reversible manner. (A) Graphic representation of the stages reached by control worms and worms treated with three different concentrations of HU (n = 18 per HU conditions, n = 14 for control condition) every day during five days. HU-treated worms showed a significantly delayed regeneration compared to that of controls. (B) Schematic representation of the experimental design used to confirm HU anti-proliferative effect: 3 dpa worms were incubated one hour with 5 µM EdU and chased in normal sea water (control; B1) or sea water with 20 mM HU (B2) for two days (until 5 dpa) before fixation. (B1-B2') EdU labelings of control worms (B1) and HU-treated worms (B2) showing a reduced number of EdU+ nuclei in HU-treated worms as compared to controls. A zoom on some nuclei of control worms (B1') shows their stippled and non-homogenous EdU labeling due to the occurrence of cell divisions during the chase period. In contrast, nuclei of HU-treated worms display a much more homogenous EdU labeling, indicative of the absence of cell divisions since EdU incorporation (B2'). Note that nuclei in HU-treated worms are slightly larger than those of control worms, which could be a consequence of HU-induced cell cycle arrest or due to the fact that worms are blocked in an earlier step of regeneration. Grey dotted lines indicate the amputation site. (C-D) Grey bars represent the timeline of the experiments and green bars the scoring days. Orange bars represent time periods during which worms were incubated in HU 20 mM in sea water, black bars time period of incubation in normal sea water (without HU). (C) On the left, schematic representation of HU treatments. On the right, graphic representation of the stages reached by the worms in the different conditions (n = 12 per HU condition, n = 16 for control condition). Significantly delayed or blocked regeneration was observed. In all conditions, worms were nevertheless able to reach at least stage 2. (D) On the left, schematic representation of HU treatments. On the right, graphic representation of the stages reached by the worms in control and five experimental conditions (n = 12 per condition). Statistics for (A), (C) and (D): 2-way ANOVA on repeated measures using Dunnett correction were done. * $p < 0.05$; * * $p < 0.01$; * * * $p < 0.001$; * * * * $p < 0.0001$. Error bar: SD.

amputation (0 dpa) and stopping it at different time points (1 to 5). As in the previous experiment, worms were scored at 5 dpa, 7 dpa and 10 dpa (Fig. 9D). In all conditions, HU treatment was reversible: after removal of HU, regeneration started again and followed a normal path in terms of stages and timing of these stages. Interestingly, worms treated from 0 to 1 dpa showed delayed segment addition and those

treated from 0 to 2 dpa delayed regeneration. This delay might reveal a certain toxicity of HU or suggest that cell proliferation, while not required to reach stage 2, could be nevertheless important during the two first days after amputation for further progression of the process.

Taken together those experiments show that intense cell proliferation occurs during *P. dumerilii* regeneration and is mandatory for regeneration to proceed beyond stage 2 of the process.

3.6. Insight into the cellular origin of the P. dumerilii regenerated region

Identifying the origin of the cells of the regenerated region is an important aspect of the understanding of a regeneration process. One question is to define whether progenitor/stem cells present before amputation may contribute to the formation of the regenerated region. Another major interrogation is to determine if the regenerated structures derive from cells located at or close to the amputation site and/or from cells migrating from more remote positions. EdU pulse and chase experiments have been widely used to indirectly tackle these questions (*e.g.*, de Jong and Seaver, 2017), even if two limitations of such experiments have to be reminded. First, only cells that were in S phase during the EdU incorporation period will be detected and stem cells that are quiescent or divide very infrequently will not be labeled. Second, during the chase period, EdU is diluted at each cell division and some daughter cells may become no more detectable at the end of the chase. Taking these elements into account, we designed EdU pulse and chase experiments to address the question of cellular origin(s) of the regenerated region during *P. dumerilii* posterior regeneration.

A first experiment was designed to test the possible involvement of primordial germ cells (PGCs) in posterior regeneration. Indeed, a recent article suggested that a cluster of cells expressing stem cell genes such as *myc* and *vasa*, located in the anterior region of the annelid *Capitella teleta*, would be the source of stem cells that migrate and contribute to posterior regeneration in this worm (de Jong and Seaver, 2017). This cluster of cells contains primordial germ cells (PGCs) that produce the *C. teleta* germ line (Dill and Seaver, 2008). PGCs expressing the aforementioned stem cell genes have also been described during early post-larval stages of *P. dumerilii* (Rebscher et al., 2007). Four PGCs are indeed produced during embryonic development by the blastomeres that also generate the larval mesodermal progenitors and the mesodermal part of the growth zone (Özpolat et al., 2017). While located in the posterior part of the body adjacent to the growth zone in late larval stages (until four days after fertilization, 4dpf), PGCs then migrate anteriorly to join a region immediately posterior to the pharynx, where these cells will start to proliferate to produce germline cells (Rebscher et al., 2007). At least during their migration, these cells express most of the stem cell genes also expressed by the posterior growth zone cells (Gazave et al., 2013). We made the hypothesis that PGCs could in fact have both germinal and somatic potentialities, producing germ cells during normal growth and sexual maturation, but being also able to contribute to posterior regeneration if amputations or injuries occur. We tested this hypothesis, by taking benefit of a previously established procedure to label these cells based on the fact that they are quiescent during embryonic and larval development and therefore retain EdU labeling (Özpolat et al., 2017; Rebscher et al., 2012). Short EdU incorporations between 5 and 7 h post fertilization (hpf) allow to label PGCs and many other cells. However, as most of these other cells subsequently divide a lot, after a chase until 48hpf or 72hpf, in the trunk of the larva, only the four PGCs show a strong and homogenous EdU labeling (Rebscher et al., 2012). We did the same incorporation, but performed a much longer chase until worms were one-month old (Fig. 10A). We found many EdU+ cells in these worms and in particular a large number of cells in one segment posterior to the pharynx (dotted line square in Fig. 10A), much likely the progeny of the PGCs. In addition, many labeled cells were also found in the head, in agreement with previously published data (Rebscher et al., 2012), and more unexpectedly also in the posterior growth zone and pygidium (Fig. 10A). To better understand this result and confirm that PGCs were labeled in this experiment, we did again EdU pulse at 5–7hpf and made chase until 3dpf, 6dpf, 10dpf and 14dpf. At 3dpf and 6dpf (Fig. 10C-D'), two groups of EdU+ cells were observed, most likely corresponding to PGCs and posterior growth zone cells (Fig. 10C'-D', arrowheads and arrows, respectively). At 10dpf and 14dpf (Fig. 10E-F'), labeled cells at the level of the posterior growth zone were still observed (arrows in Fig. 10E',F'). Strongly labeled cells were also observed in more anterior position, which correspond to the migrating PGCs (Fig. 10E,F, arrowheads). We next took 1-month worms in which PGC progeny is EdU+, amputated these worms posterior to the segment containing these cells and let the worms regenerate for three days (Fig. 10B; five worms were observed). Strikingly, the regenerated region was almost devoid of EdU+ cells, indicating that PGC progeny does not significantly contribute to regeneration, at least in this experimental design. These results do therefore not support our hypothesis that PGCs may be a source for cells of the regenerated region.

In a second experiment, we tested a possible contribution of cells that were proliferating before amputation to the formation of the regenerated region. For that purpose, we incorporated EdU during five hours immediately before amputation, which leads to the labeling of a small number of cells (Fig. S7C-C"), and put the worms after amputation in normal sea water for three to five days (Fig. S9; five worms were observed for each time point). At 3 dpa, a few labeled cells were found in the regenerated region, only in internal tissues (Fig. S9A-A'). At 5 dpa, many labeled cells are found in the lining of the regenerating gut and a few ones (very weakly labeled) in other internal tissues, likely mesodermal derivatives such as muscles (Fig. S9B-B'). No EdU+ cells were found in the epidermis neither at 3 dpa nor at 5 dpa. This experiment shows a major contribution of cells that were in S phase before amputation to the formation of the regenerated gut. Our data also suggest a much more minor contribution of such cells to regeneration of mesodermal derivatives and possibly no contribution to epidermis formation.

A third pulse and chase experiment was performed to test the involvement of cells that were proliferating after amputation (Fig. 11A). A five-hour EdU pulse was performed one day after amputation, which labeled a significant number of cells both at the amputation site, including the wound epithelium, and in all differentiated segments (Fig. 11B-B'; five worms were observed). Of note, there is no conspicuous difference in the number or distribution of the labeled cells between posterior (close to the amputation site) and anterior (more distant from the amputation site) segments (Fig. 11B). Worms were then allowed to regenerate during two days in sea water (48 h chase; worms reach 3 dpa stage; n = 5). In contrast to the previous experiment, the regenerated region contained both internal and superficial EdU labeled cells (Fig. 11C). To define whether these cells derive from cells at the amputation site, or from differentiated segments located further away, or both, we performed a second amputation. We used three different amputation planes (Fig. 11A): (i) the same plane than the first amputation (therefore we only removed the regenerated region; referred to as condition 1 below), (ii) one segment more anterior (removal of the regenerated region and the segment abutting the first amputation plane; condition 2), (iii) eight segments more anterior (removal of the regenerated region and the eight most posterior segments; condition 3). After this second amputation, worms were allowed to regenerate either three or five days in sea water (3 and 5 dpa) before EdU labeling analysis (five worms were observed for each condition and each time point). In condition 1, at 3 and 5 dpa, a large number of EdU+ cells were found both internally and superficially (prospective epidermis) (Fig. 11D,D',G,G'). In contrast, at 3 and 5 dpa, much fewer cells were EdU+ in conditions 2 and 3 and none were found in the epidermal cell layer of the regenerated region (Fig. 11E-F',H-I'). These data therefore suggest that the cells of

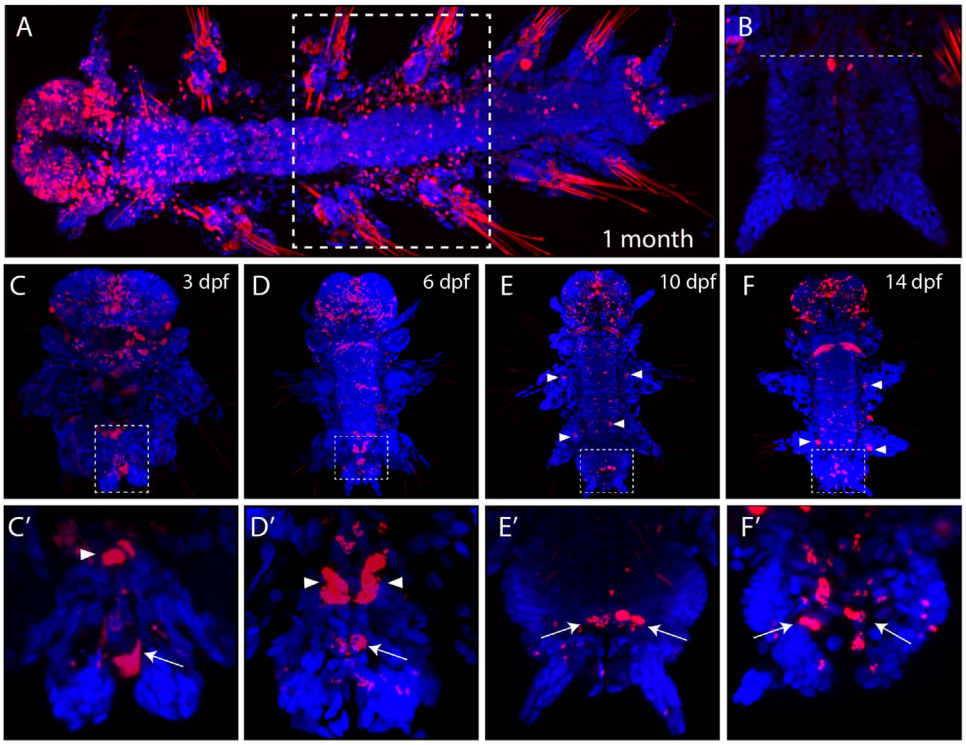

Fig. 10. Primordial germ cells do not contribute to posterior regeneration. EdU incorporation was performed from five to seven hours post fertilization and was followed by chase in normal sea water until one month post fertilization (A), three days post fertilization (3dpf; C, C'), 6dpf (D, D'), 10dpf (E, E'), or 14dpf (F, F'). EdU labeling is in red and Hoechst nuclear staining in blue. In (A) anterior is on the left. In all other images, anterior is up. (C'), (D'), (E') and (F') are higher magnification of the posterior part of the worms shown in (C), (D), (E) and (F), respectively. White arrowheads point to primordial germ cells (PGCs) and white arrows to cells of the growth zone. The dotted line square in (A) delineates the segment that contains PGC progeny. (B) Posterior part of a 1-month old worm (in which PGC daughter cells are EdU+) three days after amputation. Almost no EdU+ cells can be found in the regenerated region, indicating that PGC progeny does not significantly contribute to posterior regeneration. Grey dotted lines indicate the amputation site.

regenerated region mainly derive from cells of the segment immediately abutting the amputation site.

4. Discussion

Many animals can regenerate complex organs or body parts after an injury or an amputation. This injury-induced regeneration ability, which extends far beyond the homeostatic repair of tissues such as epidermis and intestine epithelia found in most species, is indeed very widespread in metazoans (Bely and Nyberg, 2009; Grillo et al., 2016). Highly regenerative species are found in most phyla, both non-bilaterians (such as cnidarians, ctenophores and sponges) and bilaterians including for example flatworms, annelids, arthropods, and chordates (Bely and Nyberg, 2009; Grillo et al., 2016). Regeneration has been the focus of intense research since the pioneering work of Abraham Trembley, Simon Pallas and Lazzaro Spallanzani in the 18th century (reviewed in Sánchez Alvarado, 2000). Despite this long-standing interest and the extensive study of regeneration in species such as salamanders and planarians, fundamental questions about regeneration, in particular concerning its evolution in animals, remain still unanswered. It has been advocated that solving these questions requires to study new models (or " research organisms " using the term coined by A. Sanchez Alvarado) amenable to molecular, cellular and functional analyses (Grillo et al., 2016; Sánchez Alvarado, 2018). The Errantia annelid *P. dumerilii*, which possesses extensive regenerative abilities, appears to be a particularly appropriate model to study regeneration and its evolution, thanks to its belonging to a slow-evolving lineage and the recent establishment of sophisticated molecular and genetic tools to study its development (Raible and Tessmar-Raible, 2014; Williams and Jékely, 2016; Zantke et al., 2014). In this article, we present a detailed characterization of posterior body regeneration in *P. dumerilii*, summarized in Fig. 12, which provides the essential foundation for future mechanistic and comparative studies of regeneration in this species.

4.1. Stages and timeline of P. dumerilii posterior regeneration

In P. dumerilii, amputation of the posterior part of the body leads to the removal of the posteriormost part of the body (the pygidium), the growth zone (responsible for the addition of new segments during the posterior growth of the animal) and several segments. In a couple of days, worms are able to regenerate both the differentiated structures of the pygidium and the stem cells of the growth zone which in turn allows the formation of new segments that replace the amputated ones. The whole process can therefore be subdivided into two different conceptual phases, regeneration *per se*, *i.e.*, the restoration of the pygidium and growth zone, and post-regenerative posterior growth, *i.e.*, the formation of segments by the regenerated growth zone (Gazave et al., 2013). Based on morphological observations, we defined five regeneration stages that precede the appearance of morphologically-distinguishable segments produced through post-regenerative posterior growth (Figs. 1 and 12). As far as homogenous worms in size and age are considered, the timeline of these stages appears highly reproducible, while the subsequent progressive addition of morphologically distinguishable segments is more variable. Our in-depth characterization of the different regeneration stages, using the expression of many genes involved in cell and tissue patterning and differentiation, indicates that regeneration *per se* and post-regenerative posterior growth are largely overlapping (Figs. 5 and 12). Indeed, first signs of pygidium and growth zone restoration appear two days post amputation at stage 2 and pygidium differentiation continues during the three next stages as judged by the progressive growth of the anal cirri and the progressive differentiation of the pygidial nervous system and muscles. The growth zone is regenerated between stage 2 and 3 and is

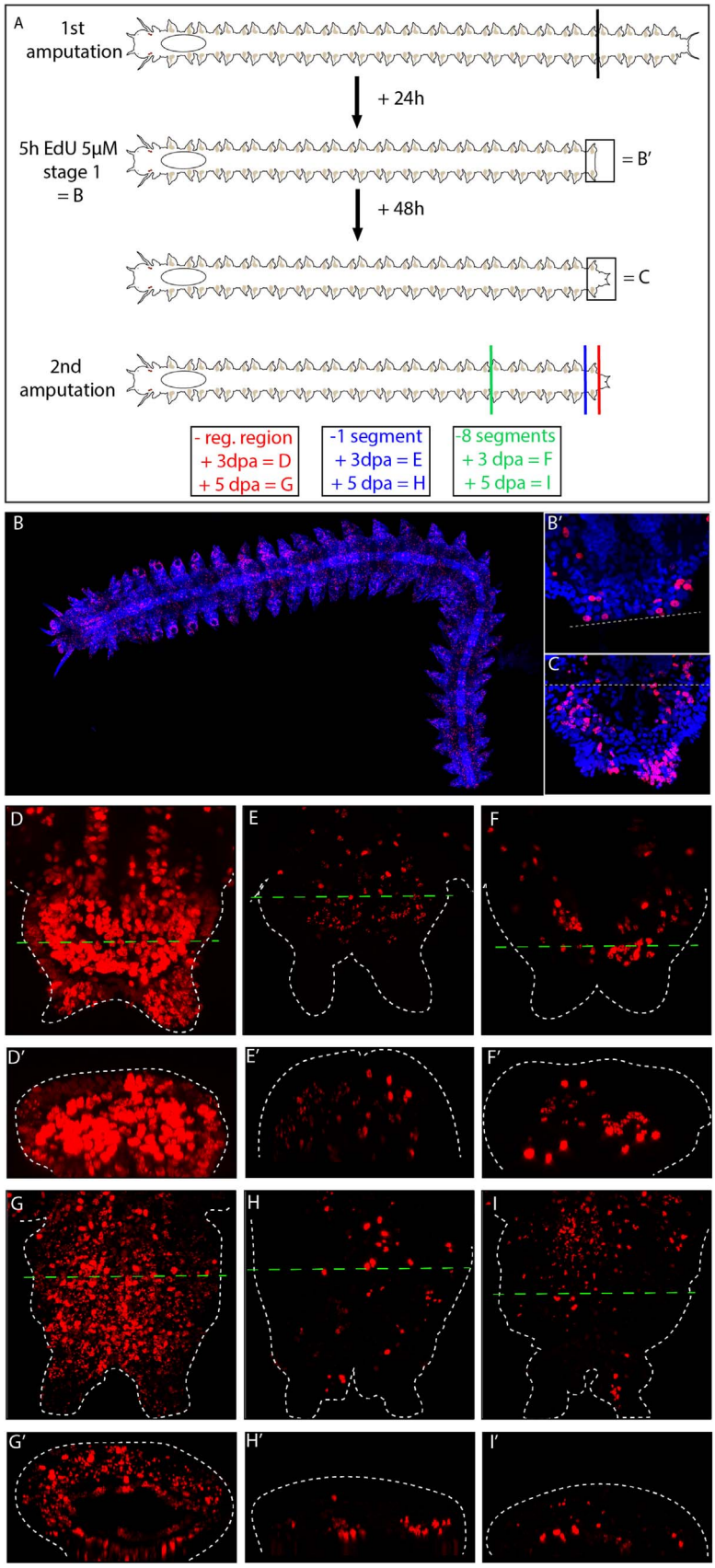
A
1st amputation
+ 24h
5h EdU 5µM stage 1 = B
= B′
+ 48h
= C
2nd amputation
- reg. region + 3dpa = D + 5 dpa = G
-1 segment + 3dpa = E + 5 dpa = H
-8 segments + 3 dpa = F + 5 dpa = I
B
B′
C
D
E
F
D′
E′
F′
G
H
I
G′
H′
I′

Fig. 11. EdU pulse and chase experiments suggest a mostly local source of cells of the regenerated region. (A) Schematic representation of the experimental design. Corresponding pictures in the lower panel are indicated. In brief, a first amputation (shown by a black bar) was performed, followed 24 h later by a 5 h EdU incorporation (5 μM). Some of the worms were fixed and imaged immediately at the end of the incorporation period (B-B'). For the others, the incorporation was followed by a 48 h chase in normal sea water. Some of the worms were fixed and imaged at the end of the chase period (C) and the others were subsequently amputated a second time. Three different amputation positions were tested (green, blue and red bars). The worms were then allowed to regenerate for either three (3 dpa, D-F') or five (5 dpa, G to I') days in normal sea water, then fixed and imaged. (B-C) EdU labeling (red) and Hoechst nuclear staining (blue). (B) Whole worm EdU labeling with 5 h EdU labeling 24 h after amputation (anterior is on the left). Many EdU+ cells are found throughout the body. (B') Higher-magnification view of the posterior part of the worm shown in (B), highlighting the presence of EdU+ cells in the regenerated region. (C) Posterior part of a worm after a 48 h chase in normal sea water. Many EdU+ cells are found in the regenerated region. (D-I') Posterior part of regenerating worms three or five days after the second amputation (D to F' and G to I', respectively) made at three different positions as schematized in (A). Green dotted lines on D-F and G-I panels indicate the position where virtual cross-sections (D' to F' and G' to I') were done. Dotted white lines show the shape of the regenerated region defined using Hoechst staining (not shown). In B', C, D to F and G to I, anterior is up; in D' to F' and G' to I', dorsal is up. Grey dotted lines indicate the amputation site.

undoubtedly functional at stage 3 (3 dpa), as shown by the addition of segment primordia at this stage (Figs. 5 and 12). In stage 4 and 5, while still not conspicuous at the morphological level, there are clearly developing segments with differentiating mesodermal and ectodermal derivatives. *P. dumerilii* posterior regeneration is therefore a very fast process and post-regenerative posterior growth starts only three days after amputation. The timeline of the process roughly corresponds to that found in other annelids, for example the other Errantia-clade species *Alitta virens* and the Sedentaria-clade species *Capitella teleta* (de Jong and Seaver, 2016; Kozin et al., 2017)

We previously studied post-regenerative posterior growth and showed that it is highly similar to the normal growth of the worms which occurs during most of its life cycle (Gazave et al., 2013). However, segment addition rate is much higher after amputation than during normal growth (Gazave et al., 2013), indicating that there is a kind of 'memory' of the fact that a part of the body has been amputated. Interestingly, we found that segment addition is more rapid if the amputation has been done more anteriorly (Fig. 2D, with the exception of amputations made too close to the pharynx). This could be interpreted in two non-mutually exclusive ways. First, if the amputation is made anteriorly, it implies that more segments are eliminated compared to more posterior amputation planes. The increase of segment addition rate could therefore be related to the fact that the worms are able to 'sense' the amount of tissues that have been deleted and to adjust their growth accordingly. Alternatively, there could be positional cues in the worm's body and it could be the position of the amputation plane with respect to these cues that defines the rate of segment addition. In agreement with this second possibility, we found that after amputation anterior parapodia (the typical appendages of annelids) regenerate faster than posterior ones (unpublished observations). In this case, the same quantity of tissue is removed by the amputation and the only difference is the position along the body axis. There is thus a clear anterior to posterior gradient of regeneration speed at least for appendages. What could be the amputation-related signals or positional cues is currently not known. An obvious candidate is the 'brain hormone' that promotes growth and inhibits reproduction in nereid annelids such as *P. dumerilii* (Schenk et al., 2016 and references therein). Concentration of this hormone progressively decreases when the worms become older and bigger. Being produced in the head, it is conceivable, but not experimentally demonstrated, that the hormone may have a graded concentration along the body axis, providing an anterior-posterior cue that can be used to control growth. In addition, there are indirect but compelling evidence that posterior amputation may lead to an increased production of the brain hormone (*e.g.*, Clark and Ruston, 1963; Scully, 1964), providing a possible explanation for the accelerated rate of growth after amputation as compared to normal non-post-traumatic growth.

4.2. *Major steps and events during* P. dumerilii *posterior regeneration*

Thomas Hunt Morgan, in the early 20th century, proposed the existence of two main modes of regeneration, epimorphosis and morphallaxis, based on whether active cell proliferation is required (epimorphic regeneration) or not (morphallactic regeneration) to ensure proper restoration of the lost body part (Morgan, 1901). Epimorphosis is by far the most common mode of regeneration and often involves the formation of a regeneration blastema (*e.g.*, Sanchez Alvarado and Tsonis, 2006). A blastema is a specialized structure

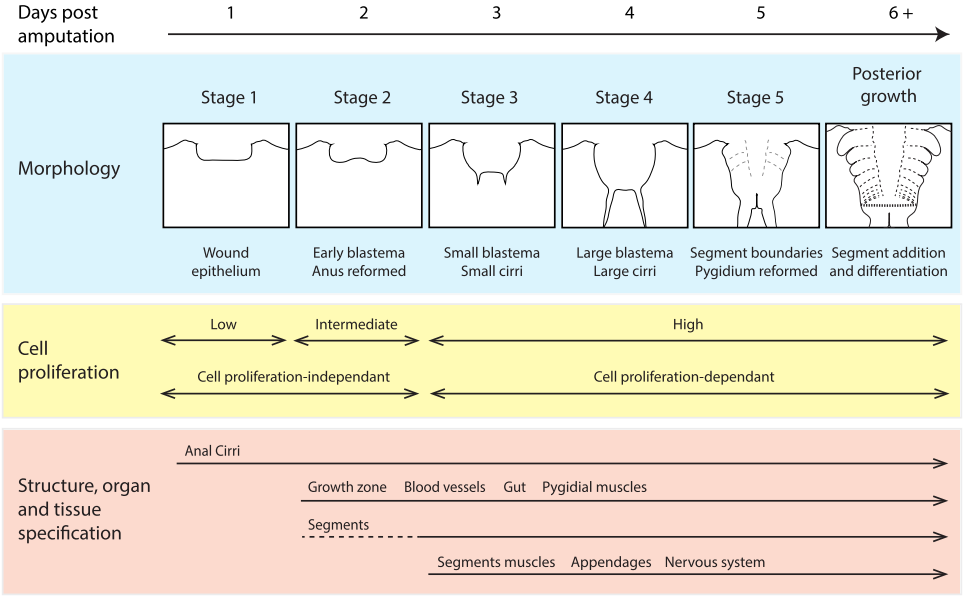

Fig. 12. Schematic summary of the main events underlying *P. dumerilii* posterior regeneration. Dotted lines in the case of 'Segments' indicate that a first band of *Pdum-engrailed* cells is observed at stage 2 that might correspond to the formation of a first segmental anlage at the border between the last differentiated segment and the regenerated region. From stage 3 onwards, additional segments are added within the regenerated region, much probably as a consequence of the activity of the growth zone.

formed upon amputation or injury and which is composed of an outer sheet of epithelial cells that covers an inner mass of mesenchyme-like cells. Regeneration is achieved by the eventual differentiation of cells of the blastema. In annelids, regeneration of the posterior body part usually is epimorphic and involves the formation of a blastema (Özpolat and Bely, 2016). In this article, we show that it is also the case in *P. dumerilii*. First, our data about expression of cell cycle genes and EdU incorporations (Fig. 8) indicate a low level of cell proliferation at stage 1, which increases at stage 2 and becomes very high from stage 3 onwards (Fig. 12). Second, we demonstrate the absolute requirement of cell divisions for proper regeneration by showing that worms treated with the anti-proliferative drug hydroxyurea (HU) are unable to fully regenerate and only reach stage 2 (Fig. 9). Finally, from stage 2 onwards, the posterior regenerated region displays a blastema-like structure with an epithelial superficial layer unsheathing an inner mass of proliferating cells. This blastema progressively gives rise in its anterior part to the growth zone and segments, and in its posterior part to the pygidium and its characteristic outgrowths, the anal cirri (Figs. 1, 5 and 8).

Similar characteristic steps and events have been described during epimorphic regeneration in several annelids (Özpolat and Bely, 2016). Hereafter we describe when and how they occur in *P. dumerilii*.

4.2.1. Wound healing

As in other annelids, this step is rapidly achieved in *P. dumerilii* (one day or less) and first involves the contraction of muscles at the amputation site, then followed by the formation of a wound epithelium (Figs. 6 and S4). Few proliferating cells are found in the wound epithelium (as well as throughout the worm's body; Figs. 8 and S7) and HU treatments indicate that cell proliferation is not required for wound healing (Fig. 9). Several genes are strongly expressed in wound epithelium (Fig. 5), including genes encoding transcription factors (*Pdum-hox3*, *Pdum-evx*, *Pdum-engrailed*, *Pdum-ap2* and *Pdum-prdm3/16*), signaling molecules (*Pdum-wnt1* and *Pdum sfrp1/2/5*), or RNA-binding proteins (*Pdum-elav*). Several other genes are expressed in mesodermal cells of the segment immediately adjacent to the amputation site (Figs. 5 and 7). This includes several 'stem cells genes' belonging to the germline multipotency program (GMP), already shown to be expressed during early regeneration stages in other annelids (*e.g.*, Kozin and Kostyuchenko, 2015; Özpolat and Bely, 2015). Interestingly, most of the genes expressed in wound epithelium or adjacent mesodermal tissues, are more strongly or exclusively expressed on the ventral side of the worm, indicating the existence of dorso-ventral cues at this early regeneration stage. *Pdum-elav* shows a particularly striking expression (Fig. 5K), being only expressed in the ventralmost part of the wound epithelium which abuts the ventral nerve cord (VNC), suggesting that its expression might be induced by signals from the VNC. This would be consistent with the hypothesis that *P. dumerilii* regeneration, like that of many other species (reviewed in Boilly et al., 2017a), could be nerve-dependent.

4.2.2. Blastema formation

A blastema-like organization is found in *P. dumerilii* from 2 dpa onwards. At this stage more important cell proliferation is observed (Fig. 8), but HU treatments indicate that this stage can be reached when cell divisions are blocked (Fig. 9). Intense and broad expression of 'stem cells genes' are found in the blastema, mainly in its internal mesenchymal-like cells (Fig. 7). An obvious and important question is the fate of the blastemal cells and in particular whether they may have stem cell properties. The expression of homologs of genes such as *piwi*, *vasa*, *nanos* and *myc* may be viewed as suggestive of a stem cell identity for the blastemal cells. However, caution should be taken as these genes are also expressed in non-stem cells, for example during *P. dumerilii* posterior growth in segmental mesodermal and ectodermal progenitors (Gazave et al., 2013). Only cell lineage tracing experiments will allow to safely define the fate of the cells of the blastema.

4.2.3. Blastema patterning

As already mentioned, dorso-ventral differences in gene expressions are observed as early as in stage 1 (1 dpa). During the following stages, many of the genes we have studied show differential expression along this axis (Figs. 5, 7 and S3). Most stem cell genes are, for example, more strongly and broadly expressed on the ventral side than on the dorsal side. Cell proliferation is also more intense on the ventral side (Fig. 8). While we do not have experimental data in *P. dumerilii* about what could control dorso-ventral organization during regeneration, elegant surgical manipulations in *Nereis pelagica*, which is phylogenetically closely-related to *P. dumerilii*, have provided evidence for a role of the VNC (reviewed in Boilly et al., 2017b). Indeed, when the VNC is absent from the wound site, regeneration occurs, but the aneurogenic regenerated region seems to be only composed of dorsal tissues (*e.g.*, Boilly and Combaz, 1970; Boilly-Marer and Combaz, 1972), suggesting that signals from the VNC are required for the formation of ventral tissues. Anterior-posterior organization of the *P. dumerilii* blastema is also established at early stages. Indeed, at stage 2 (2 dpa), some genes, such as *Pdum-wnt1* and *Pdum-dlx* are expressed in the posteriormost part of the blastema while others, such as *Pdu-engrailed* and *Pdum-ap2*, are expressed in its anterior part (Figs. 5 and 7). From stage 3 onwards, a clear demarcation between the posterior pygidium and more anterior growth zone and developing segments is obvious at the levels of gene expression and cell proliferation. How blastema anterior-posterior polarity is controlled is currently not known. An obvious positional cue could be linked to the fact that the anterior part of the blastema is in contact with cells of the last remaining differentiated segments while its posterior part does not.

4.2.4. Tissue differentiation

Earliest signs of differentiation, or at least commitment of cells towards a particular differentiated state, are observed at stage 2 (2 dpa; Fig. 12). Indeed, at this stage, a loosely-organized gut is present (Fig. 1) and some cells in the posterior part of the blastema express *Pdum-twist* (Fig. 5), suggesting that these cells are already engaged to produce pygidial muscles. Phalloidin staining suggests that some of these muscles already start to differentiate (Fig. 6). At stage 3, additional expression of *Pdum-twist* is found in the anterior blastema part, from which segments will be formed, and muscle differentiation occurs at the following stages (Figs. 6 and 7). At stages 2 and 3, cells expressing *Pdum-prdm3/16* are observed and are likely blood vessels progenitors (Fig. 5). Well distinguishable ventral and dorsal blood vessels are observed from stage 4 onwards (Fig. 5). At stage 3, nervous system formation starts as seen by the expression of genes such as *Pdum-pax6* and *Pdum-neurogenin* (Fig. 5). A complex and well organized VNC and nerves are observed both in the developing segment and pygidium from stage 4 onwards (Fig. 6). Finally developing parapodia, expressing genes such as *Pdum-dlx*, are present from stage 3 onwards (Fig. 5).

4.3. Insights into the cellular origin of the P. dumerilii blastema

Identifying the cellular source(s) of the cells of the regenerated region is an important aspect in the understanding of a regeneration process. This in fact covers two distinct questions. One of these interrogations is whether blastemal cells are produced by divisions of pre-existing stem cells or derive from differentiated cells through dedifferentiation and/or transdifferentiation events, or by a combination of both. The other question is whether the regenerated region is solely produced by cells at, or close to, the amputation site, or may involve the migration of cells from more distant positions. The two aspects are often mixed together by opposing two hypotheses about blastema formation, local dedifferentiation *versus* migration of stem cells from different parts of the body. We however have to keep in mind that migratory cells are not necessarily stem cells and that there could

be stem cells located at the amputation site. A third important question is whether different parts of the blastema, ectodermal, mesodermal and endodermal derivatives, have similar or distinct origins, and thus whether pluripotent stem or progenitor cells may be involved in regeneration.

One way to distinguish stem cells from differentiated cells is that the former might be proliferating while the latter usually do not. We therefore performed EdU incorporations before amputation to label cells that divide irrespectively of amputation, then amputated the worms and let them regenerate for three or five days (Fig. S9). Only few EdU+ cells are found in the regenerated region at 3 dpa and only internal labeled cells are observed. At 5 dpa, very strikingly, almost all EdU+ are in the intestinal lining and a large number of gut cells are in fact EdU+. These results indicate that the regenerating intestine mostly or exclusively derives from cells that were proliferative before amputation. A plausible hypothesis is that the *P. dumerilii* gut, like that of other animals, contains stem cells normally involved in the homeostatic replacement of the gut epithelium, but which can, upon injury, also allow its regeneration (*e.g.*, Forsthoefel et al., 2011; Gehart and Clevers, 2015). Our results also suggest that cells proliferating before amputation do not importantly contribute to the regeneration of mesodermal derivatives and might not contribute at all to that of epidermis. It is however important to note that our experiments do not demonstrate that ectodermal and mesodermal cells do not derive from stem cells, as these cells could be quiescent before amputation (and therefore not labeled by EdU incorporations) and re-enter cell cycle as a consequence of injury.

To address the question of blastemal cells origin, we designed another EdU pulse and chase experiment. In this case, we labeled cells whose division was stimulated by amputation by incorporating EdU at 1 dpa and we next performed a two-day chase, amputated the worms a second time and let them regenerate for three or five days (Fig. 11). Importantly, the second amputation was made at three different positions, similar plane than the first one, or one or eight segments more anteriorly. When the same amputation plane was used (the differentiated segment that abuts the first amputation site was left in place), the regenerated part formed after the second amputation contains many EdU+ cells, which were found both in the superficial and internal layers of the blastema. In contrast, in the experiments with the two other amputation planes, which have in common that the differentiated segment abutting the first amputation site was eliminated by the second amputation, only few EdU+ cells were found in the blastema after the second amputation and few or none of these cells were superficial. These results suggest that the blastema would mostly derive from cells located in the segment immediately adjacent to the amputation site, with no major contribution to blastema formation of cells migrating from distant segments. These results will nevertheless have to be confirmed and refined in the future by other approaches, in particular cell lineage tracing experiments.

We also tested if primordial germ cell (PGC) progeny could have a role in posterior regeneration. Indeed, these cells were shown to express a collection of stem cells genes, which constitutes the germline multipotency program (GMP), also expressed by the posterior growth zone cells which whom PGCs share a common embryonic progenitor origin (Gazave et al., 2013; Özpolat et al., 2017; Rebscher et al., 2007). PGCs, which produce the germ cells, could therefore also have somatic potentialities in particular in a regenerative context. Using a previously published way to label PGCs (Rebscher et al., 2012) and combining this labeling with amputation, we were able to show that PGCs, at least in our experimental design, do not contribute to blastema formation (Fig. 10). Similarly, a study in another annelid, *Enchytraeus japonensis*, also suggested that germ line stem cells do not contribute to regeneration of somatic tissues (Tadokoro et al., 2006).

Taken together, our data suggest a mostly local origin of the blastema in *P. dumerilii*. Our results also suggest that gut cells may have a different origin than mesodermal and ectodermal derivatives. Our data are fully consistent with observations and experiments made in other annelids (reviewed in Bely, 2014), in particular those made in the 60 s on other Errantia annelids by Bénoni Boilly (*e.g.*, Boilly, 1965a, 1965b; Boilly, 1968a, 1968b, 1968c; Boilly, 1969a, 1969b, 1969c). His careful histological and electron microscopy observations, combined with experimental manipulations, indeed strongly suggested that blastemal cells form through dedifferentiation events and that the different germ layers of the regenerated region have distinct origins. In addition, targeted destructions of cells of different segments have indicated that only the cells of the segment abutting the amputation site were required for regeneration.

5. Conclusions

In conclusion, we performed a thorough morphological, cellular and molecular characterization of posterior regeneration in the annelid *P. dumerilii*. We showed that this process involves the formation of a regeneration blastema and provide evidence for the importance of cell proliferation for proper regeneration. The cells of the blastema express from early stages a collection of genes known to be markers of pluripotent/ multipotent stem cells, suggesting that the blastema may contain such cells with high potency. Our data also suggest that blastemal cells mostly derive from cells of the segment adjacent to the amputation site. Taken together, our data pave the way for further analysis of *P. dumerilii* regeneration, and, ultimately, through comparative analyses, for a better understanding of the evolution of regeneration in animals.

Acknowledgements

We thank all Vervoort lab members for helpful discussions and feedback on the manuscript. We are grateful to Aldine Amiel, Bénoni Boilly, Christine Rampon and Eric Röttinger for helpful suggestions and discussions. We thank Patricia Alvarez-Campos and Thibault Bidolet for help with some *in situ* hybridizations, and Pierre Kerner for careful reading of the manuscript and for providing *Pdum-Prdm3/16* probe. We acknowledge the ImagoSeine facility (member of the France BioImaging infrastructure supported by the Agence Nationale de la Recherche, ANR-10-INSB-04, “Investments of the future”) and its experienced staff for their assistance in confocal imaging. Animal facility members are thanked for their help with the worm culture. This work was supported by funding from Labex ‘Who Am I’ laboratory of excellence (No. ANR-11-LABX-0071) funded by the French Government through its ‘Investments for the Future’ program operated by the Agence Nationale de la Recherche under grant No. ANR-11-IDEX-0005-01, Centre National de la Recherche Scientifique, and Agence Nationale de la Recherche (grant TELOBLAST no. ANR-16-CE91-0007). JP wishes to thank M. Candás and Xela Cunha-Veira (Estación de Bioloxía Mariña-EBMG, Universidade de Santiago, Spain) and Cati Sueiro and Ada Castro (Servizos de Apóio á Investigación-SAI, Universidade da Coruña, Spain) for their help with use of the microCT and SEM, respectively. Both imaging techniques were financially supported by the project Fauna Ibérica X: Polychaeta VI: Palpata-Canalipalpata I (CGL2014–53332-C5-3-P) from the Ministry of Economy, Industry and Competitiveness (Spain).

Appendix A. Supplementary material

Supplementary data associated with this article can be found in the online version at doi:10.1016/j.ydbio.2018.11.004.

References

Alba-Tercedor, J., Sánchez-Tocino, L., 2011. The use of the SkyScan 1172 high-resolution micro-CT to elucidate if the spicules of the sea slugs (Mollusca: Nudibranchia, Opisthobranchia) have a structural or a defensive function. SkyScan

Users Meet. 2011, 113–121.
Audouin, J.V., Milne, Edwards H., 1833. Classification des Annélides et description de celles qui habitent les côtes de la France. Ann. des Sci. Nat. Paris 29, 195–269.
Bastin, B.R., Chou, H.-C., Pruitt, M.M., Schneider, S.Q., 2015. Structure, phylogeny, and expression of the frizzled-related gene family in the lophotrochozoan annelid Platynereis dumerilii. EvoDevo 6, 37. http://dx.doi.org/10.1186/s13227-015-0032-4.
Bely, A.E., 2014. Early events in annelid regeneration: a cellular perspective. Integr. Comp. Biol. 54, 688–699. http://dx.doi.org/10.1093/icb/icu109.
Bely, A.E., Nyberg, K.G., 2009. Evolution of animal regeneration: re-emergence of a field. Trends Ecol. Evol. (Amst.). http://dx.doi.org/10.1016/j.tree.2009.08.005.
Boilly, B., 1965a. Origine du mésoderme dans la régénération postérieure chez Syllis amica Quatrefages (Annélide Polychète). Comptes Rendus De. l'Académie Des. Sci. Paris 261, 1561–1564.
Boilly, B., 1965b. Localisation des cellules de régénération chez Nereis diversicolor O. F. Muller (Annélide Polychète). Comptes Rendus De. l'Académie Des. Sci. Paris 261, 2009–2011.
Boilly, B., 1968a. Origine des cellules de régénération chez Aricia foetida Clap. (Annélide Polychète). Arch. D.'Anat. Microsc. 57, 297–308.
Boilly, B., 1968b. Etude ultrastructurale de l'évolution des tissus impliqués dans la régénération céphalique et caudale de Syllis amica Q. (Annélide Polychète): I. La dédifférenciation. J. Microsc. 7, 865–876.
Boilly, B., 1968c. Etude ultrastructurale de l'évolution des tissus impliqués dans la régénération céphalique et caudale de Syllis amica Q. (Annélide Polychète): II. L'activation et la différenciation. J. Microsc. 7, 877–894.
Boilly, B., 1969a. Etude expérimentale de la localisation, par rapport au plan d'amputation, de la source des cellules de régénération mésodermiques chez une Annélide Polychète Syllis amica Quatrefages. J. Embryol. Exp. Morph 21, 193–206.
Boilly, B., 1969b. Origine des cellules régénératrices chez Nereis diversicolor O. F. Muller (Annélide Polychète). Wilhelm. Roux' Arch. 162, 286–305.
Boilly, B., 1969c. Sur l'origine des cellules régénératrices chez les annélides polychètes. Arch. Zool. Exp. Gen. 110, 127–143.
Boilly, B., Faulkner, S., Jobling, P., Hondermarck, H., 2017a. Nerve Dependence: from Regeneration to Cancer. Cancer Cell 31, 342–354. http://dx.doi.org/10.1016/j.ccell.2017.02.005.
Boilly, B., Boilly-Marer, Y., Bely, A.E., 2017b. Regulation of dorso-ventral polarity by the nerve cord during annelid regeneration: a review of experimental evidence. (doi.org/)Regen. (Oxf., Engl.) 4, 54–68. http://dx.doi.org/10.1002/reg2.78.
Boilly, B., Combaz, A., 1970. Influence de la chaine nerveuse sur la régénération caudale de *Nereis diversicolor* O.F. Muller (Annélide Polychète). Comptes Rendus De. l'Académie Des. Sci. Paris 271, 92–95.
Boilly-Marer, Y., Combaz, A., 1972. Différenciation aneurale de papilles pygidiales chez une *Heteronereis* (*Nereis pelagica* L. (Annélide Polychète). Comptes Rendus De. l'Académie Des. Sci. Paris 274, 1693–1696.
Chou, H.C., Acevedo-Luna, N., Kuhlman, J.A., Schneider, S.Q., 2018. PdumBase: a transcriptome database and research tool for *Platynereis dumerilii* and early development of other metazoans. BMC Genom. 19, 618. http://dx.doi.org/10.1186/s12864-018-4987-0.
Clark, R.B., Ruston, R.J., 1963. Time of release and action of a hormone influencing regeneration in the polychaete *Nereis diversificolor*. General. Comp. Endocrinol. 3, 542–553.
de Jong, D.M., Seaver, E.C., 2017. Investigation into the cellular origins of posterior regeneration in the annelid Capitella teleta. Regen. (Oxf.) 5, 61–77. http://dx.doi.org/10.1002/reg2.94.
de Jong, D.M., Seaver, E.C., 2016. A Stable Thoracic Hox Code and Epimorphosis Characterize Posterior Regeneration in Capitella teleta. PLoS One 11, e0149724. http://dx.doi.org/10.1371/journal.pone.0149724.
de Rosa, R., Prud'homme, B., Balavoine, G., 2005. Caudal and even-skipped in the annelid Platynereis dumerilii and the ancestry of posterior growth. Evol. Dev. 7, 574–587. http://dx.doi.org/10.1111/j.1525-142X.2005.05061.x.
Demilly, A., Steinmetz, P., Gazave, E., Marchand, L., Vervoort, M., 2013. Involvement of the Wnt/β-catenin pathway in neurectoderm architecture in *Platynereis dumerilii*. Nat. Comm. 4, 1915. http://dx.doi.org/10.1038/ncomms2915.
Denes, A.S., Jékely, G., Steinmetz, P.R.H., Raible, F., Snyman, H., Prud'homme, B., Ferrier, D.E.K., Balavoine, G., Arendt, D., 2007. Molecular architecture of annelid nerve cord supports common origin of nervous system centralization in bilateria. Cell 129, 277–288. http://dx.doi.org/10.1016/j.cell.2007.02.040.
Dill, K.K., Seaver, E.C., 2008. *Vasa* and *nanos* are coexpressed in somatic and germ line tissue from early embryonic cleavage stages through adulthood in the polychaete *Capitella* sp. I. Dev. Genes Evol. 218, 453–463. http://dx.doi.org/10.1007/s00427-008-0236-x.
Dorresteijn, A.W.C., O'Grady, B., Fischer, A., Porchet-Henere, E., Boilly-Marer, Y., 1993. Molecular specification of cell lines in the embryo of Platynereis (Annelida). Roux's arch. Dev. Biol. 202, 264–273.
Fincher, C.T., Wurtzel, O., de Hoog, T., Kravarik, K.M., Reddien, P.W., 2018. Cell type transcriptome atlas for the planarian Schmidtea mediterranea. (pii: eaaq1736) Science 360. http://dx.doi.org/10.1126/science.aaq1736.
Fischer, A.H., Henrich, T., Arendt, D., 2010. The normal development of Platynereis dumerilii (Nereididae, Annelida). Front Zool. 7, 31. http://dx.doi.org/10.1186/1742-9994-7-31.
Forsthoefel, D.J., Park, A.E., Newmark, P.A., 2011. Stem cell-based growth, regeneration, and remodeling of the planarian intestine. Dev. Biol. 356, 445–459. http://dx.doi.org/10.1016/j.ydbio.2011.05.669.
Gazave, E., Béhague, J., Laplane, L., Guillou, A., Préau, L., Demilly, A., Balavoine, G., Vervoort, M., 2013. Posterior elongation in the annelid Platynereis dumerilii involves stem cells molecularly related to primordial germ cells. Dev. Biol. 382, 246–267. http://dx.doi.org/10.1016/j.ydbio.2013.07.013.
Gazave, E., Lemaître, Q.I.B., Balavoine, G., 2017. The Notch pathway in the annelid Platynereis: insights into chaetogenesis and neurogenesis processes. Open Biol., 7. http://dx.doi.org/10.1098/rsob.160242.
Gehart, H., Clevers, H., 2015. Repairing organs: lessons from intestine and liver. Trends Genet. 31, 344–351. http://dx.doi.org/10.1016/j.tig.2015.04.005.
Grillo, M., Konstantinides, N., Averof, M., 2016. Old questions, new models: unraveling complex organ regeneration with new experimental approaches. Curr. Opin. Genet. Dev. 40, 23–31. http://dx.doi.org/10.1016/j.gde.2016.05.006.
Grimmel, J., Dorresteijn, A.W.C., Fröbius, A.C., 2016. Formation of body appendages during caudal regeneration in Platynereis dumerilii: adaptation of conserved molecular toolsets. EvoDevo 7, 10. http://dx.doi.org/10.1186/s13227-016-0046-6.
Herlant-Meewis, H., 1964. Regeneration in annelids. Adv. Morphog. 4, 155–215.
Janssen, R., Le Gouar, M., Pechmann, M., Poulin, F., Bolognesi, R., Schwager, E.E., Hopfen, C., Colbourne, J.K., Budd, G.E., Brown, S.J., Prpic, N.-M., Kosiol, C., Vervoort, M., Damen, W.G.M., Balavoine, G., Mcgregor, A.P., 2010. Conservation, loss, and redeployment of Wnt ligands in protostomes: implications for understanding the evolution of segment formation. BMC Evol. Biol. 10, 374. http://dx.doi.org/10.1186/1471-2148-10-374.
Juliano, C.E., Swartz, S.Z., Wessel, G.M., 2010. A conserved germline multipotency program. Development 137, 4113–4126. http://dx.doi.org/10.1242/dev.047969.
Kerner, P., Degnan, S.M., Marchand, L., Degnan, B.M., Vervoort, M., 2011. Evolution of RNA-binding proteins in animals: insights from genome-wide analysis in the sponge Amphimedon queenslandica. Mol. Biol. Evol. 28, 2289–2303. http://dx.doi.org/10.1093/molbev/msr046.
Knapp, D., Tanaka, E.M., 2012. Regeneration and reprogramming. Curr. Opin. Genet. Dev. 22, 485–493. http://dx.doi.org/10.1016/j.gde.2012.09.006.
Kozin, V.V., Filippova, N.A., Kostyuchenko, R.P., 2017. Regeneration of the Nervous and Muscular System after Caudal Amputation in the Polychaete *Alitta virens* (Annelida: nereididae). Russ. J. Dev. Biol. 48, 198–210. http://dx.doi.org/10.1134/S1062360417030079.
Kozin, V.V., Kostyuchenko, R.P., 2015. Vasa, PL10, and Piwi gene expression during caudal regeneration of the polychaete annelid Alitta virens. Dev. Genes Evol. 225, 129–138. http://dx.doi.org/10.1007/s00427-015-0496-1.
Morgan, T.H., 1901. Regeneration. The Macmillan Company, New York.
Myohara, M., 2012. What role do annelid neoblasts play? A comparison of the regeneration patterns in a neoblast-bearing and a neoblast-lacking enchytraeid oligochaete. PLoS ONE 7, e37319. http://dx.doi.org/10.1371/journal.pone.0037319.
Özpolat, B.D., Handberg-Thorsager, M., Vervoort, M., Balavoine, G., 2017. Cell lineage and cell cycling analyses of the 4d micromere using live imaging in the marine annelid Platynereis dumerilii. Elife, 6. http://dx.doi.org/10.7554/eLife.30463.
Özpolat, B.D., Bely, A.E., 2016. Developmental and molecular biology of annelid regeneration: a comparative review of recent studies. Curr. Opin. Genet. Dev. 40, 144–153. http://dx.doi.org/10.1016/j.gde.2016.07.010.
Özpolat, B.D., Bely, A.E., 2015. Gonad establishment during asexual reproduction in the annelid Pristina leidyi. Dev. Biol. 405, 123–136. http://dx.doi.org/10.1016/j.ydbio.2015.06.001.
Pfeifer, K., Schaub, C., Wolfstetter, G., Dorresteijn, A., 2013. Identification and characterization of a twist ortholog in the polychaete annelid Platynereis dumerilii reveals mesodermal expression of Pdu-twist. Dev. Genes Evol.. http://dx.doi.org/10.1007/s00427-013-0448-6.
Poss, K.D., 2010. Advances in understanding tissue regenerative capacity and mechanisms in animals. Nat. Rev. Genet 11, 710–722. http://dx.doi.org/10.1038/nrg2879.
Prud'homme, B., de Rosa, R., Arendt, D., Julien, J.-F., Pajaziti, R., Dorresteijn, A.W.C., Adoutte, A., Wittbrodt, J., Balavoine, G., 2003. Arthropod-like expression patterns of engrailed and wingless in the annelid Platynereis dumerilii suggest a role in segment formation. Curr. Biol. 13, 1876–1881. http://dx.doi.org/10.1016/j.cub.2003.10.006.
Raible, F., Tessmar-Raible, K., 2014. Platynereis dumerilii. Curr. Biol. 24, R676–R677. http://dx.doi.org/10.1016/j.cub.2014.06.032.
Rebscher, N., Lidke, A.K., Ackermann, C.F., 2012. Hidden in the crowd: primordial germ cells and somatic stem cells in the mesodermal posterior growth zone of the polychaete Platynereis dumerillii are two distinct cell populations. EvoDevo 3, 9. http://dx.doi.org/10.1186/2041-9139-3-9.
Rebscher, N., Zelada-González, F., Banisch, T.U., Raible, F., Arendt, D., 2007. Vasa unveils a common origin of germ cells and of somatic stem cells from the posterior growth zone in the polychaete Platynereis dumerilii. Dev. Biol. 306, 599–611. http://dx.doi.org/10.1016/j.ydbio.2007.03.521.
Reddien, P.W., 2013. Specialized progenitors and regeneration. Development 140, 951–957. http://dx.doi.org/10.1242/dev.080499.
Sánchez Alvarado, A., 2018. To solve old problems, study new research organisms. Dev. Biol. 433, 111–114. http://dx.doi.org/10.1016/j.ydbio.2017.09.018.
Sanchez Alvarado, A., Tsonis, P.A., 2006. Bridging the regeneration gap: genetic insights from diverse animal models. Nat. Rev. Genet. 7, 873–884. http://dx.doi.org/10.1038/nrg1923.
Sánchez Alvarado, A., 2000. Regeneration in the metazoans: why does it happen? Bioessays 22, 578–590.
Schenk, S., Krauditsch, C., Frühauf, P., Gerner, C., Raible, F., 2016. Discovery of methylfarnesoate as the annelid brain hormone reveals an ancient role of sesquiterpenoids in reproduction. Elife 5, 44. http://dx.doi.org/10.7554/eLife.17126.
Scully, U., 1964. Factors influencing the secretion of regeneration-promoting hormone in Nereis diversicolor. General. Comp. Endocrinol. 4, 91–98.
Simionato, E., Kerner, P., Dray, N., Le Gouar, M., Ledent, V., Arendt, D., Vervoort, M., 2008. atonal- and achaete-scute-related genes in the annelid Platynereis dumerilii: insights into the evolution of neural basic-Helix-Loop-Helix genes. BMC Evol. Biol.

8, 170. http://dx.doi.org/10.1186/1471-2148-8-170.
Struck, T.H., Paul, C., Hill, N., Hartmann, S., Hösel, C., Kube, M., Lieb, B., Meyer, A., Tiedemann, R., Purschke, G., Bleidorn, C., 2011. Phylogenomic analyses unravel annelid evolution. Nature 471, 95–98. http://dx.doi.org/10.1038/nature09864.
Tadokoro, R., Sugio, M., Kutsuna, J., Tochinai, S., Takahashi, Y., 2006. Early segregation of germ and somatic lineages during gonadal regeneration in the annelid *Enchytraeus japonensis*. Curr. Biol. 16, 1012–1017. http://dx.doi.org/10.1016/j.cub.2006.04.036.
Tanaka, E.M., 2016. The Molecular and Cellular Choreography of Appendage Regeneration. CELL 165, 1598–1608. http://dx.doi.org/10.1016/j.cell.2016.05.038.
Tanaka, E.M., Reddien, P.W., 2011. The cellular basis for animal regeneration. Dev. Cell 21, 172–185. http://dx.doi.org/10.1016/j.devcel.2011.06.016.
Tessmar-Raible, K., Steinmetz, P.R., Snyman, H., Hassel, M., Arendt, D., 2005. Fluorescent two-color whole mount in situ hybridization in Platynereis dumerilii (Polychaeta, Annelida), an emerging marine molecular model for evolution and development. Biotechniques 39, 460–464.
Vervoort, M., Meulemeester, D., Béhague, J., Kerner, P., 2016. Evolution of Prdm Genes in Animals: insights from Comparative Genomics. Mol. Biol. Evol. 33, 679–696. http://dx.doi.org/10.1093/molbev/msv260.
Wagner, D.E., Wang, I.E., Reddien, P.W., 2011. Clonogenic neoblasts are pluripotent adult stem cells that underlie planarian regeneration. Science 332, 811–816. http://dx.doi.org/10.1126/science.1203983.
Williams, E.A., Jékely, G., 2016. Towards a systems-level understanding of development in the marine annelid Platynereis dumerilii. Curr. Opin. Genet. Dev. 39, 175–181. http://dx.doi.org/10.1016/j.gde.2016.07.005.
Zakrzewski, A.-C., Weigert, A., Helm, C., Adamski, M., Adamska, M., Bleidorn, C., Raible, F., Hausen, H., 2014. Early divergence, broad distribution, and high diversity of animal chitin synthases. Genome Biol. Evol. 6, 316–325. http://dx.doi.org/10.1093/gbe/evu011.
Zattara, E.E., Turlington, K.W., Bely, A.E., 2016. Long-term time-lapse live imaging reveals extensive cell migration during annelid regeneration. BMC Dev. Biol. 16, 6. http://dx.doi.org/10.1186/s12861-016-0104-2.
Zantke, J., Bannister, S., Rajan, V.B.V., Raible, F., Tessmar-Raible, K., 2014. Genetic and Genomic Tools for the Marine Annelid Platynereis dumerilii. Genetics 197, 19–31. http://dx.doi.org/10.1534/genetics.112.148254.
Zeng, A., Li, H., Guo, L., Gao, X., McKinney, S., Wang, Y., Yu, Z., Park, J., Semerad, C., Ross, E., Cheng, L.C., Davies, E., Lei, K., Wang, W., Perera, A., Hall, K., Peak, A., Box, A., Sánchez Alvarado, A., 2018. Prospectively isolated tetraspanin(+) neoblasts are adult pluripotent stem cells underlying planaria regeneration. Cell 173, 1593–1608. http://dx.doi.org/10.1016/j.cell.2018.05.006.